

Water Quality Assessment Simulation Program (WASP8): Upgrades to the Advanced Toxicant Module for Simulating Dissolved Chemicals, Nanomaterials, and Solids



Water Quality Assessment Simulation Program (WASP8): Upgrades to the Advanced Toxicant Module for Simulating Dissolved Chemicals, Nanomaterials, and Solids

CSS 10.04 Emerging Materials

Project Leads: William Boyes and Dermont Bouchard

Task 3: Develop Predictive Modeling and Tools

Task Leads: Dermont Bouchard and Paul Harten

QA Category: Level 4 (Category B)

Computational Exposure Division

Athens, GA

Authors

Robert B. Ambrose, Jr., Emeritus, USEPA, Office of Research and Development, Athens, GA

Brian Avant, ORISE, USEPA, Office of Research and Development, Athens, GA

Yanlai Han, Ph.D., ORISE, USEPA, Office of Research and Development, Athens, GA

Christopher D. Knightes, Ph.D., USEPA, Office of Research and Development, Athens, GA

Tim Wool, USEPA, Region 4, Atlanta, GA

Disclaimer

This document has been reviewed in accordance with U.S. Environmental Protection Agency policy and approved for publication. Mention of trade names or commercial products does not constitute endorsement or recommendation for use.

Table of Contents

1.0	Introduction	1
2.0	The Advanced Toxicant Module.	2
3.0	Solids Transport	3
3.1	Introduction	3
3.2	Theory.	3
3.2.1	Solids Systems	3
3.3	Implementation	3
3.4	Water Body Compartments	4
3.4.1	Stream Sedimentation Regimes	4
3.5	Descriptive Solids Transport	4
3.6	Process Based Solids Transport.	5
3.7	Biotic Solids Production and Dissolution	7
3.8	Solids Burial	7
3.9	Analytical Solution for Settling.	8
3.10	Example	9
4.0	Light	11
4.1	Introduction	11
4.2	Theory.	11
4.2.1	Light Attenuation	11
4.3	Implementation	11
4.3.1	Input Total Radiation	11
4.3.2	Light Attenuation Above Water Surface	12
4.3.3	Light Attenuation Below the Water Surface	12
5.0	Particle Attachment	14
5.1	Introduction	14
5.2	Theory.	14
5.2.1	Equilibrium Sorption.	14
5.2.2	Kinetic Sorption	15
5.2.3	Nanomaterial Heteroaggregation	15
5.3	Implementation	15
5.3.1	Equilibrium Sorption.	15
5.3.2	Kinetic Sorption	16
5.3.3	Nanomaterial Heteroaggregation	16
6.0	Nanomaterial Reactions	17
6.1	Introduction	17
6.2	Nanomaterial Reactions.	17
6.2.1	General Reactions Module	17
6.2.2	Effect of Temperature	18
6.2.3	Phase Multiplication Factor	18
6.2.4	Segment Multiplication Factor.	18
6.2.5	Monod Kinetics	18
6.2.6	Environmental Kinetics	18
6.3	Nanomaterial Phototransformation	18
6.4	Implementation	19
6.5	Examples	19
6.5.1	Silver Nanoparticles Dissolution.	19
6.5.2	Calculation of Nanomaterial Phototransformation Rate Constants	19
6.5.3	Nanomaterial Parallel Reaction	21
6.5.4	Segment Multiplication Factor.	21
6.5.5	Phase Multiplication Factor	21

7.0	Dissolved Chemicals Reactions	23
7.1	Introduction	23
7.2	Simulation for Oxidation, Reduction and Biodegradation	23
7.2.1	Generic Reaction Module	23
7.2.2	Effect of Temperature	23
7.2.3	Phase Multiplication Factor	23
7.2.4	Segment Multiplication Factor	23
7.2.5	Monod Kinetics	24
7.2.6	Environmental Kinetics	24
7.2.7	Second Order Kinetics	24
7.2.8	Biodegradation	24
7.3	Dissolved Chemicals Phototransformation	24
7.4	Examples	24
7.4.1	First-Order Biodegradation Influenced by Temperature	24
7.4.2	Second-Order Reaction	25
8.0	References	26
9.0	APPENDIX	A-1
9.1	Solids QA/QC	A-1
9.1.1	Scenario 1 – Constant Boundary Conditions, Initial Concentration = 0, No Settling	A-1
9.1.2	Scenario 2 - Initial Conditions, Boundary Condition = 0, No Settling	A-2
9.1.3	Scenario 3 – Initial Concentration, With and Without Streamflow, Settling.	A-2
9.1.4	Scenario 4 - Resuspension	A-3
9.2	Light QA/QC	A-4
9.2.1	Option 0, Calculated Diel Light	A-5
9.2.2	Option 1, User Input Diel Light	A-6
9.2.3	Option 2, User Input Daily Light, Calculated Diel Light	A-7
9.3	Particle Attachment QA/QC	A-9
9.3.1	Equilibrium Sorption.	A-9
9.3.2	Kinetic Sorption	A-9
9.3.3	Nanomaterial Heteroaggregation	A-11

List of Figures

Figure 1. Stream Sedimentation Regimes	4
Figure 2 Noncohesive erosion and resuspension	6
Figure 3. Solids Concentration in the Surface Water	9
Figure 4. Solids Concentration in the Surface Sediments	10
Figure 5. Solids Concentration in the Subsurface Sediments	10
Figure 6. Sediment Burial Rates	10
Figure 7 Possible Nanomaterial Reaction Pathways. Chem indicates dissolved chemicals (e.g., organics, metal ion).	17
Figure 8. (a) [Ag] experimental data and WASP8 simulation results, (b) $[Ag^+]_{\text{released}}$ experimental data and WASP8 simulation results.	20
Figure 9. Nanomaterial parallel reaction pathways.	21
Figure 10. Nanomaterial parallel reaction simulation results using WASP8	21
Figure 11. WASP8 simulation results.	22
Figure 12. WASP8 output of biodegradation rate at different temperatures, fitted with analytical solution	25
Figure 13. Second-order reaction simulation results by WASP8.	25
Figure 14. Comparison of WASP Simulation to Analytical Solution for Scenario 1	A-1
Figure 15. Comparison of WASP Simulations to Analytical Solutions for Scenario 2	A-2
Figure 16. Comparison of WASP Simulations to Analytical Solutions for Scenario 3, With Streamflow	A-2
Figure 17. Comparison of WASP Simulations to Analytical Solutions for Scenario 3, Without Streamflow	A-3
Figure 18. Comparison of WASP Simulations to Analytical Solutions for Scenario 4, Solids in Sediment Layer.	A-4
Figure 19. Comparison of WASP Simulations to Analytical Solutions for Scenario 4, Solids in Water Column	A-4
Figure 20. Comparison of Analytical Solution and WASP Simulation for Sorption Kinetics of Scenario 1. Chem 1 represents the freely dissolved chemical concentration, and Chem 2 represents the chemical concentration sorbed to the suspended solid.	A-10
Figure 21. Comparison of Analytical Solution and WASP Simulation for Sorption Kinetics of Scenario 2. Chem 1 represents the freely dissolved chemical concentration, and Chem 2 represents the chemical concentration sorbed on the suspended solid.	A-10
Figure 22. Comparison of Analytical Solution and WASP Simulated Nanoparticle Concentration over Time for Scenario 1	A-12

List of Tables

Table 1. Particle size classification	3
Table 2. Particle densities	3
Table 3. Channel Geometry of WASP Segments	9
Table 4. Solids Demonstration Parameters	9
Table 5. WASP Default Light Extinction Coefficients for the Wavelength Bands	13
Table 6. Division of Wavelengths by Wave Class.	13
Table 7. Division of Wavelengths into Wave Bands, with Fractions Given by Latitude	13
Table 8. Equilibrium Sorption Parameters	14
Table 9. Data retrieved from publication and WASP8 simulated results	20
Table 10. Wavelength-dependent reaction rate of each wavelength band	20
Table 11. Parameters used in Analytical Equations	A-1
Table 12. Channel Geometry of WASP Segment	A-1
Table 13. Physical properties of solids	A-2
Table 14. Channel Geometry of WASP Segments	A-4
Table 15. Attenuation Fractions Used for Above Surface Parameters	A-4
Table 16. Average K_c Outputs for Each Attenuation Parameter by Light Group	A-5
Table 17. WASP Outputs by Wavelength Group for Option 0 Using Athens, GA Coordinates	A-5
Table 18. Comparison of WASP Outputs to Analytical Solutions for Above Surface Light Attenuation – Option 0	A-5
Table 19. Comparison of WASP Outputs to Analytical Solutions for Below Surface Light Attenuation – Option 0	A-6
Table 20. Comparison of WASP Outputs to Analytical Solutions for Below Surface Light Attenuation – Option 0	A-6
Table 21. Comparison of WASP Outputs to Analytical Solutions for Above Surface Light Attenuation – Option 1	A-6
Table 22. Comparison of WASP Outputs to Analytical Solutions for Below Surface Light Attenuation – Option 1	A-7
Table 23. Comparison of WASP Outputs to Analytical Solutions for Below Surface Light Attenuation – Option 1	A-7
Table 24. WASP Outputs by Wavelength Group for Option 2 Using Athens, GA Coordinates	A-7
Table 25. Comparison of WASP Outputs to Analytical Solutions for Above Surface Light Attenuation – Option 2	A-8
Table 26. Comparison of WASP Outputs to Analytical Solutions for Below Surface Light Attenuation – Option 2	A-8
Table 27. Comparison of WASP Outputs to Analytical Solutions for Below Surface Light Attenuation – Option 2	A-8
Table 28. Variables Related to Equilibrium Sorption	A-9
Table 29. Parameter Values and Results for each Scenario	A-9
Table 30. Sorption Kinetic Constants and Analytical Errors of Two Scenarios	A-9
Table 31. Heteroaggregation Kinetics Parameters	A-11
Table 32. Channel Geometry of WASP Segment	A-11
Table 33. Calculated Rate of Collision by Mechanism	A-11
Table 34. Parameters for Different Cases of α for Brownian Motion Scenario.	A-12
Table 35. Parameters for Different Cases of α for Brownian Motion and Fluid Motion Scenario	A-12
Table 36. Calculated and Simulated Nanoparticle Concentrations Using Different Alphas	A-13
Table 37. Analytic Solutions for Heteroaggregation Constants Using	A-13
Table 38. Nanoparticle Concentrations Using Different Alphas	A-13

1.0

Introduction

The Water Quality Analysis Simulation Program (WASP) is a dynamic, spatially-resolved, differential mass balance fate and transport modeling framework. WASP is used to develop models to simulate concentrations of environmental contaminants in surface waters and sediments. As a modeling framework, it allows users to construct the model design that is appropriate for the system of interest, in one, two, or three dimensions. WASP allows for time-varying processes of advection, dispersion, point and diffuse mass loading, boundary conditions and boundary exchange. WASP can be linked to hydrodynamic and sediment transport models, or the hydrodynamic algorithms within the WASP framework can be used. WASP is one of the most widely used water quality models in the USA and throughout the world. It has been applied in development of Total Maximum Daily Loads (TMDLs)^{1,2}; simulation of nutrients in Tampa Bay, FL³; and remediation strategies for mercury in the Sudbury River, MA^{4,5}.

WASP is an enhancement of the original version developed in the 1980s⁶⁻⁸. Over the years, it has undergone many improvements and enhancements. In July 2017, WASP8 (WASP, v.8.1) was released. It was a complete overhaul and recoding that moved from Fortran77 to Fortran95 to take advantage of many updated features. This release also incorporated a new WASP interface, a new post-processor (WRDB), and the ability to run on a PC or Mac.

WASP8 contains two modules: the Advanced Eutrophication module and the Advanced Toxicant module. These provide the tools to simulate different environmental contaminants of concern. Advanced Eutrophication simulates conventional pollutants (e.g., dissolved oxygen, nitrogen, algae). Over the years, much of WASP's development focused on the eutrophication module, details that are not part of this document. Similarly, the overall workings of WASP, such as

how to construct a WASP model or how to simulate flow, are not included. The focus here is on the Advanced Toxicant module's recent advances.

WASP's Toxicant module (WASP TOXI, WASP7 and earlier) originally focused on dissolved organic contaminants, with the capacity to model metals in a descriptive manner and simulate solids. The new Advanced Toxicant module in WASP8 was completely rewritten to advance it from being able to simulate three chemicals and three solids (generally, sands, fines, and particulate organic matter). WASP8 now permits simulation of seven state variables: dissolved chemicals, nanomaterials, solids, dissolved organic carbon, temperature, salinity, and bacteria. For each variable, the number of how many can be simulated is pre-set (e.g., up to 10 chemicals); due to the new architecture, these can be increased with small adjustments in the source code, by request.

As part of the upgrade to WASP8, and the incorporation of nanomaterials as a new state variable, we present here an overview of the theory and application of:

- Solids Transport
- Light and Phototransformations
- Particle Attachment
- Nanomaterial Transformation Reactions
- Chemical Transformation Reactions

Each topic is discussed by providing an introduction; the theory of the topic with equations used to describe the processes; implementation of this module within WASP; and specific examples in some cases. Quality assurance/quality control (QA/QC) tests to verify that incorporation of these processes into WASP match analytical results are presented in Appendix A.

2.0

The Advanced Toxicant Module

The WASP8 Advanced Toxicant Module is structured to provide flexibility in constructing the processes that govern the contaminant(s) of interest. The user selects the type of state variables and number of each. The type of contaminants that WASP8 can simulate, ranging from simple to more complex, are shown below.

- Metals
 - Copper, Lead, Zinc, Cadmium
 - Arsenic, Tin, Selenium, Chromium
- Mercury
 - Elemental, Divalent, Methyl (Explicit Mercury Model to Be Released)
- Organics
 - MTBE, PCB Homolog
 - Petroleum, BTEX, PAHs, Chlorinated Solvents, VOCs
 - Pesticides, Organic Acids
- Nanomaterials
 - Carbon Nanotubes, Graphene Oxide, Titanium Dioxide, Silver Sulfide

WASP8's Advanced Toxicant Module is a noticeable advance over WASP7. The types and numbers of state variables now include:

Dissolved Chemicals	(n = 1 to 10+)
Nanomaterials	(n = 1 to 10+)
Solids	(n = 1 to 10+)
Dissolved Organic Carbon	(n = 1 to 5+)
Bacteria	(n = 1 to 5+)
Temperature	(n = 1)
Salinity	(n = 1)

The maximum number of variables for each class of state variable is set as a limit in the code, however, it can be updated by adjusting and recompiling the source code.

We discuss the three main state variables of dissolved chemicals, nanoparticles, and solids. Solids are particularly important for simulating toxicants because they provide a surface for attachment. Their transport is governed by associated particles. Light governs phototransformations of dissolved chemicals and nanoparticles, so we incorporate the new way that WASP handles light and phototransformations. Simulation of Dissolved Organic Carbon, Bacteria, Temperature, and Salinity are not incorporated here, as it is beyond the scope of this effort. Some processes governing chemicals are also left out (e.g., volatilization). Details on how to simulate these will be incorporated as develop the user's guide documents that is part of the WASP executable.

3.0 Solids Transport

3.1. Introduction

Suspended and benthic solids are important components of water quality. Excess suspended solids concentrations can harm fish directly through direct mortality, or by reducing their growth rate and resistance to disease. High concentrations increase light attenuation and surface heating; the consequential reductions in light affect algal growth rates and abundance of food available to fish. Excess silts can blanket benthic spawning areas and damage invertebrates. Organic deposits can reduce dissolved oxygen levels, causing an imbalance in natural biota.

Solids affect conventional water quality through sorption of nutrients. Sorption reduces dissolved ammonia (NH₄) and phosphate (PO₄) fractions, reducing nitrification and algal uptake and growth. Particulate nutrient fractions are removed from the water column by deposition, and returned by erosion and resuspension.

Solids also affect the fate of potential toxicants, including organic chemicals and nanomaterials. Sorption reduces their dissolved fraction and bioavailability, and deposition removes them from the water column, attenuating some peak loading events. Net deposition stores chemicals in sediments for long periods. Pore water diffusion and resuspension return chemicals to the water column between loading events. Large flood events scour significant amounts of sediment and chemical from the upper sediment to the water column. Burial below bioturbation depth potentially sequesters chemicals from biota.

The solids module is an independent set of routines for the solids state variable. It has its own set of associated Constants, Parameters, and Time Functions and is implemented as a unit within each of these modules.

Like other state variables, Solids are transported between segments by advection and dispersion. They can also settle through the water column; deposit to the surface benthic (sediment) layer; erode and resuspend back to the water column; and bury to lower benthic layers. These processes are described below. Using the Solids Option in the Constants section, Solids Transport group, you can choose the descriptive option (0) or one of the process-based solids transport options (1 or 2) for each Solid system.

3.2. Theory

3.2.1. Solids Systems

WASP8 can simulate up to 10 different Solids systems, each representing a discrete size range and density. You must choose how many solids types to simulate, and then specify their characteristic sizes and densities. Table 1 gives characteristic size ranges for different classes of solids. Table 2 gives typical densities.

Table 1. Particle size classification⁹

Size Range	Wentworth Name	Common Name
1 to 100 nm	nanoparticle	nanoparticle
< 1 μm	colloid	mud
1.0 – 3.9 μm	clay	mud
3.9 – 62.5 μm	silt	mud
62.5 - 125 μm	very fine sand	sand
125 - 250 μm	fine sand	sand
0.25 – 0.5 mm	medium sand	sand
0.5 – 1 mm	coarse sand	sand
1 – 2 mm	very coarse sand	sand
2 – 4 mm	granule	gravel
4 – 64 mm	pebble	gravel
64 – 256 mm	cobble	gravel
> 256 mm	boulder	gravel

Table 2. Particle densities¹⁰

Substance	Density [g/mL]
Organic matter (dry weight)	1.27
Siliceous minerals	2.65
Garnet sands	4.0

3.3. Implementation

Solids are specified in the Systems section. Each row is an independent model system. Enter new rows by clicking the ‘Insert’ button or by setting the cursor to the bottom row and pressing the keyboard’s down arrow. To specify a solids variable, double-click a cell in the System Type column and select “SOLID”; a default name is provided in the System Name column. You can specify a more descriptive name by double-clicking a cell in that column.

Particle densities are also specified in the Systems section. The Density column is preset to 1.0 g/mL, the nominal density of water. WASP8 will reset the particle density to 2.65 g/mL if you do not specify an alternate density.

The characteristic particle diameter for each Solid is specified in the Constants section, Solids Transport group. WASP8 will assign a default value of 0.025 mm, which is characteristic of silt, if you do not specify particle diameter.

3.4. Water Body Compartments

WASP8 model networks are composed of spatially-discrete segments, or compartments. Detailed network segmentation is best generated with special WASP builder software linked to GIS platforms such as BASINS (<https://www.epa.gov/exposure-assessment-models/basins>). Simple networks can be specified directly in the WASP8 user interface.

Each segment is represented by a row in the Segments section of the interface. Segments are specified in the Segment Type column, and consist of four types:

- Surface Water
- Subsurface Water
- Surface Benthic
- Subsurface Benthic

The Transport Mode determines how advective transport through each segment is calculated. This is covered in the WASP8 Advective Flow document.

For networks with vertical discretization, map segments vertically, using the Segment Below column. The default setting is “None,” indicating there is no model segment immediately below the current one. To specify a segment below, double-click in the cell and select the proper segment from a pick list. WASP8 will internally map the segments in vertical columns.

The water column – The water column is composed of Surface Water and Subsurface Water segments, linked by advective flow paths and dispersive exchanges.

The sediment bed – Sediment beds are layers composed of Surface Benthic and Subsurface Benthic segments, arranged in vertical stacks beneath a water column segment. Each segment is defined by its bulk density, porosity, cohesiveness and organic content. These properties are not specified directly in WASP8, but are a product of the simulated individual solids systems with their properties.

The initial total solids concentration in a benthic segment [mg/L or g/m³] sets the reference bulk density [g/mL] and porosity [L_w/L]. As described in Section 3.8, the solids mass balance preserves reference bulk densities and porosities for benthic segments when individual solids are added or removed. Initial concentrations are specified in the Segments section, Initial Conditions group.

A benthic segment is considered “non-cohesive” or “cohesive” based on whether the fraction of clay and silt-size solids (those less than 0.10 mm) exceeds the specified critical fraction. You can specify the “Critical cohesive sediment fraction, above which bed acts cohesively” in the Constants section, Solids Transport group; the default value is 0.2. In cohesive beds, clay and silt particles are eroded as a unit, but eroded separately in non-cohesive beds.

3.4.1. Stream Sedimentation Regimes

The transport of solids in surface waters is governed to a large degree by particle size and stream velocity (or bottom shear stress).

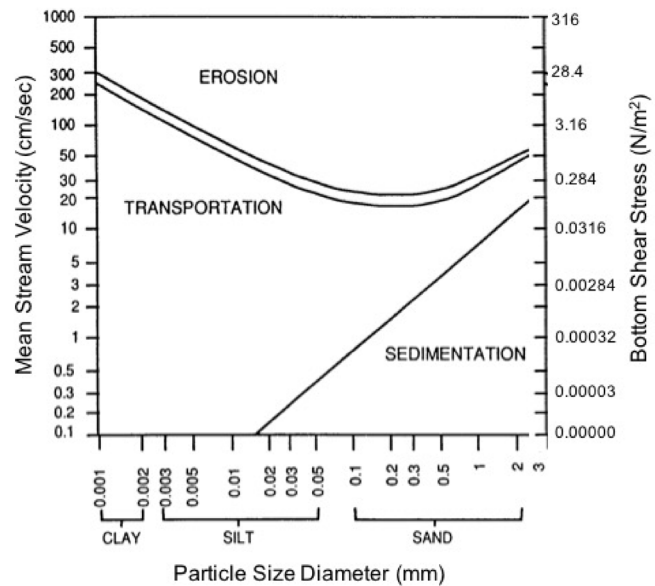


Figure 1. Stream Sedimentation Regimes

3.5. Descriptive Solids Transport

If default Solids Option 0 is chosen for a Solid system, WASP8 will apply segment-specific settling and resuspension velocities as shown in the Parameter Data section, Solids group. Settling is the movement of a solid from one water column segment to the underlying water column segment. Deposition is the transfer of a solid from a water column segment to the underlying surface benthic segment. Resuspension is the transfer of a solid from a surface benthic segment to the overlying water column segment. Solids burial is calculated internally, based on mass balance calculations for total solids within the benthic segments.

Settling and Deposition – The Solids Settling Velocity w_s [m/d] should be specified for settling or deposition from each water column segment. WASP multiplies w_s by the solids concentration in the segment [g/m³] to obtain the solids flux [g/m²-d] to the segment below. Note that the deposition velocity for a solid is generally a fraction of the characteristic settling velocity for that solid, as described in the *Deposition* subsection in Section . In WASP8, Solids Transport constants can be specified to make deposition dependent on shear stress. For Solids Option 0, the default values for these deposition constants are set so that specified settling velocities will be used for deposition.

Note that settling and deposition velocities can be quite high for size classes from coarse silts and above, causing severe numerical burdens. When settling removes more than 0.1% of a solid from a water column segment during the calculation time step, WASP8 uses an analytical solution described in Appendix 1. The calculates C^* [g/m³], the average solid concentration during the time step; this concentration is used in the WASP8 solution for settling and advection out of the segment during the time step.

Resuspension – The Solids Resuspension Velocity, w_R [m/d], should be specified for resuspension from each surface benthic segment. WASP multiplies w_R by the solids concentration in the segment [g/m^3] to obtain the solids flux [$\text{g}/\text{m}^2\text{-d}$] to the segment above.

3.6. Process Based Solids Transport

If Solids Option 1 or 2 is chosen, WASP8 will use a set of solids constants, along with process-based equations to calculate dynamic settling, deposition, erosion, and resuspension velocities. While settling is a function of particle size and density, deposition, erosion, and resuspension are functions of bottom shear stress. Erosion and resuspension also depend on whether the sediment bed is acting cohesively or noncohesively. Solids burial is calculated internally based on mass balance calculations for total solids within the benthic segments, which is described in Section 3.8.

Bottom Shear Stress – Flowing water exerts a shear stress, τ_b [N/m^2], on the benthic surface layer. WASP8 uses the Darcy–Weisbach expression for the grain-related bottom shear stress (skin friction) that is a function of the average water velocity, u [m/s], and water density, ρ_w [kg/m^3]:

$$\tau_b = \frac{\rho_w f u^2}{8} \quad \text{Equation 1}$$

f is the Darcy–Weisbach friction factor, estimated by:

$$f = \frac{0.24}{\log^2(12 \frac{H}{k_s})} \quad \text{Equation 2}$$

where H is water depth [m], D_{50} is median sediment grain size [m], and k_s is the equivalent roughness height [m], calculated as $3D_{50}$ or $0.01H$, whichever is larger. Note that for a bed of medium sand (0.5 mm), or finer, in streams greater than 5 cm deep, f assumes a constant value of 0.0253. With values of ρ_w close to $998 \text{ kg}/\text{m}^3$, the bottom shear stress simplifies to:

$$\tau_b = 3.16u^2 \quad \text{Equation 3}$$

Settling – Settling is the movement of solids down through the water column. WASP8 calculates the settling velocity, w_s [m/s], for each solid using the van Rijn (1984) method. This set of equations is based on mean particle diameter, D_s [m], particle density, ρ_s [kg/m^3], water density, ρ_w [kg/m^3], and absolute viscosity, μ [$\text{kg}/\text{m}\cdot\text{s}$]:

$$\frac{w_s}{\sqrt{g'D_s}} = \begin{cases} \frac{R_d}{18} & D \leq 100\mu\text{m} \\ \frac{10}{R_d} \left(\sqrt{1 + 0.01R_d^2} - 1 \right) & 100\mu\text{m} < D \leq 1000\mu\text{m} \\ 1.1 & D > 1000\mu\text{m} \end{cases} \quad \text{Equation 4}$$

where R_d is the sediment particle densimetric Reynolds number:

$$R_d = \frac{D_s \sqrt{g'D_s}}{\mu/\rho_w} \quad \text{Equation 5}$$

and

$$g' = g \left(\frac{\rho_s}{\rho_w} - 1 \right) \quad \text{Equation 6}$$

where g is the acceleration of gravity, $9.807 \text{ [m}/\text{sec}^2]$. For $D_s < 100 \mu\text{m}$ (very fine sands and smaller), the van Rijn expression reduces to Stokes' Law:

$$w_s = \frac{D_s^2}{18\mu} g(\rho_s - \rho_w) \quad \text{Equation 7}$$

For $D_s > 1000 \mu\text{m}$ (very coarse sands and larger), and particle density of $2650 \text{ kg}/\text{m}^3$, the van Rijn expression simplifies to:

$$w_s = 4.425\sqrt{D_s} \quad \text{Equation 8}$$

In the model initialization phase, WASP8 calculates the characteristic settling velocity for each simulated solid using the input particle densities and diameters, along with nominal values for water viscosity ($0.001 \text{ kg}/\text{m}\cdot\text{s}$) and water density ($1000 \text{ kg}/\text{m}^3$).

Deposition – Deposition is the movement of solids from the water column to the surficial benthic (or sediment) bed. In noncohesive deposition, the settling of individual solids particles is attenuated by the shear stress from water flow. WASP8 calculates the deposition velocity, w_D [m/s], for each solid as the product of its settling velocity, w_s , and probability of deposition upon contact with bed, a_D :

$$w_D = w_s a_D \quad \text{Equation 9}$$

where a_D is a function of bottom shear stress, τ_b , as well as the lower and upper critical shear stress thresholds, τ_{cd1} and τ_{cd2} . Using a formulation by Krone (1963), a_D is equal to 1 for $\tau_b < \tau_{cd1}$, and equal to 0 for $\tau_b > \tau_{cd2}$. Within the critical shear stress range, a_D varies from 1 to 0 as bottom shear stress rises from τ_{cd1} to τ_{cd2} in a roughly linear fashion:

$$a_D = \left(\frac{\tau_{cd2} - \tau_b}{\tau_{cd2} - \tau_{cd1}} \right)^{\gamma_D} \quad \text{Equation 10}$$

where τ_{cd1} and τ_{cd2} are in [N/m^2], and γ_D is a dimensionless exponent. For the default g_D of 1.0, the interpolation function is linear.

These three constants are input for each solid in the Constants section, Solids Transport group. The lower critical shear stress for deposition is generally considered to be close to $0.0 \text{ N}/\text{m}^2$, while the upper critical shear stress for deposition is in the range of $0.01 - 0.2 \text{ N}/\text{m}^2$, depending on particle size. For Solids Options 1 and 2, the default values for τ_{cd1} and τ_{cd2} are set to 0.0 and $0.2 \text{ N}/\text{m}^2$. For Solids Option 0, they are set to 10 and $20 \text{ N}/\text{m}^2$ so that, under all reasonable conditions, deposition is set to the specified settling velocity.

Noncohesive Erosion – Noncohesive erosion is the detachment of solids particles from the surface benthic sediment into a mobile boundary layer. Resuspension is the transport of the solids particles from the mobile layer into the water column (Figure 2). In noncohesive benthic segments, all solids particles are subject to noncohesive erosion and resuspension. In cohesive benthic segments, only sands and larger particles ($> 0.1 \text{ mm}$ diameter) are subject to noncohesive erosion and resuspension.

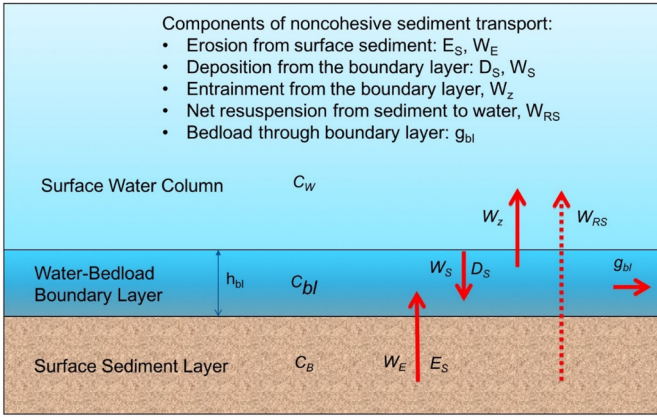


Figure 2 - Noncohesive erosion and resuspension

In WASP8, erosion velocity and flux are calculated for each particle size class using either the van Rijn or Roberts formulation (Solids option 1 or 2). These are based on particle diameter and density, the bottom shear stress, and the critical shear stress for erosion.

The van Rijn erosion algorithm (Solids Option 1) calculates a non-dimensional quantity, E , which is the ratio of the gross erosion to gross deposition rate. The erosion velocity, then, is the product of E and the settling velocity:

$$W_E = E W_S \quad \text{Equation 11}$$

The van Rijn non-dimensional E is:

$$E = 0.015 \gamma_E \frac{D_s}{k_s} R_d^{-0.2} \tau_*^\eta \quad \text{Equation 12}$$

where γ_E is a user-specified multiplier that defaults to 1.0 D_s is the median particle size [m], k_s is the roughness height [m], R_d is the sediment particle densimetric Reynolds number (defined above), η is a user-specified exponent that defaults to 1.5, and τ_* is the non-dimensional shear stress:

$$\tau_* = \frac{\tau_b - \tau_{cE}}{\tau_{cE}} \quad \tau_b \geq \tau_{cE} \quad \text{Equation 13}$$

$$\tau_* = 0 \quad \tau_b < \tau_{cE} \quad \text{Equation 14}$$

where τ_b is the bottom shear stress [N/m^2] and τ_{cE} is the critical shear stress for erosion:

$$\tau_{cE} = \gamma_{cE} (\rho_s - \rho_w) g D_s \theta_{cE} \quad \text{Equation 15}$$

where γ_{cE} is a user-specified multiplier that defaults to 1.0 and θ_{cE} is the non-dimensional Shields parameter, which is calculated by the Brownlie (1981) fit to the Shields curve:

$$\theta_{cE} = 0.22 R_d^{-0.6} + 0.06 \times 10^{-7.7 R_d^{-0.6}} \quad \text{Equation 16}$$

The critical velocity for erosion, u_{cE} [m/s], is the velocity that produces τ_{cE} :

$$u_{cE} = \sqrt{8 \tau_{cE} / \rho_w f} \quad \text{Equation 17}$$

In WASP8, calibrate van Rijn noncohesive erosion by specifying values for the following constants in the Solids Transport group: shear stress exponent for noncohesive resuspension, h (default = 1.5); critical shear stress multiplier

for noncohesive resuspension, γ_{cE} (default = 1.0), and shear stress multiplier for noncohesive resuspension, γ_E (default = 1.0).

Eroded solids in the mobile boundary layer may be transported along the sediment bed by bed load, or to the water column by resuspension.

The Roberts erosion algorithm (Solids Option 2) calculates erosion velocity w_E [m/s] for each particle size class as a function of bottom shear stress τ_b [N/m^2] and bulk density ρ_B [kg/m^3]:

$$w_E = \gamma_E A \rho_B^m \tau_b^n \quad \text{Equation 18}$$

where γ_E is a user-specified multiplier that defaults to 1.0. The fitting coefficients A , m , and n were determined experimentally for different particle sizes from fine silt (less than 5.7 μm) to coarse sand (greater than 1.25 mm). In WASP8, you can calibrate the Roberts erosion rate by specifying a value for the shear stress multiplier for noncohesive resuspension, γ_E (default = 1.0) in the Solids Transport group.

Noncohesive Resuspension – Noncohesive resuspension is the transport of the solids particles from the mobile layer or from the surface benthic segment into the water column (Figure 2). Eroded particles move in the boundary layer as bed load below the critical shear stress for resuspension, ρ_{cRS} [N/m^2].

$$\tau_{cRS} = 0.1 \frac{(4 w_s 100 / D_s)^2}{\rho_w / 1000} \quad \text{Equation 19}$$

where w_s is the settling velocity [m/s], ρ_w is the water density [kg/m^3], and D_s is the non-dimensional particle diameter, given by

$$D_* = \left[\frac{(\rho_s - \rho_w) g}{\rho_w \nu^2} \right]^{1/3} D_s \quad \text{Equation 20}$$

When bottom shear stress exceeds τ_{cRS} , particles are entrained from the mobile boundary layer and resuspension begins. The net resuspension velocity w_R is given by:

$$W_R = f_{RS} W_E \quad \text{Equation 21}$$

where f_{RS} is the fraction of the noncohesive erosion that is entrained to suspension, given by:

$$f_{RS} = 0 \quad \tau_b < \tau_{cRS} \quad \text{Equation 22}$$

$$f_{RS} = \frac{\ln(u_* / w_s) - \ln(u_{*cRS} / w_s)}{\ln(4) - \ln(u_{*cRS} / w_s)} \quad \tau_b \geq \tau_{cRS} \quad \text{Equation 23}$$

$$f_{RS} = 1 \quad u_* \geq 4 w_s \quad \text{Equation 24}$$

where u_* is shear velocity [m/s], u_{*cRS} is critical shear velocity for resuspension [m/s], and w_s is particle settling velocity [m/s]. The shear velocity and critical shear velocity are given by:

$$u_* = \sqrt{\tau_b / \rho_w} \quad \text{Equation 25}$$

$$u_{*cRS} = \sqrt{\tau_{cRS} / \rho_w} \quad \text{Equation 26}$$

Noncohesive Bed Load – Bed load is the transport of noncohesive solids particles downstream through the mobile layer. Bed load begins when the bottom shear stress exceeds the critical shear stress for erosion, τ_{cE} . Most eroded particles are redeposited back to the surface sediment layer. The bed load flux per unit width, g_{bl} [g/m-s] is given by the van Rijn expression:

$$g_{bl} = \alpha_{bl} \rho_s u h \left(\frac{D_{s0}}{h} \right)^{1.2} M_e^n \quad \text{Equation 27}$$

where α_{bl} is a fitted coefficient, u is stream velocity [m/s], h is depth [m], h is a fitted exponent, and M_e is given by:

$$M_e = \frac{u - u_{cE}}{\sqrt{\left(\frac{\rho_s - \rho_w}{\rho_w} \right) g D_{s0}}} \quad \text{Equation 28}$$

where u_{cE} is the critical velocity for erosion, given in the previous section.

van Rijn calibrated the bed load flux equation to measured transport data (van Rijn, 2007), yielding $\alpha_{bl} = 15$ and $n = 1.5$. In WASP8, α_{bl} is given by:

$$\alpha_{bl} = 15 * vBLmult \quad \text{Equation 29}$$

where $vBLmult$ is the calibration multiplier for bed load flux (default = 1.0) and h is set to $vRNonCohExp$, the shear stress exponent for noncohesive resuspension (default = 1.5). Both are specified in the Constants section, Solids Transport group.

Cohesive Resuspension – Cohesive erosion is the detachment and transfer of a thin layer of cohesive sediment from the surface benthic sediment to the water column. All cohesive solids in the eroded layer are transferred at the erosion velocity, w_E [m/s].

A commonly-used expression for cohesive erosion flux [g/m²-s] is the following excess shear stress power law formulation (Lick et al., 1994):

$$E_{coh} = f_{coh} M \tau_*^n \quad \text{Equation 30}$$

where M is the shear stress multiplier [g/m²-s], n is the shear stress exponent, f_{coh} is the fraction of the surface bed that is cohesive, and τ_* is the excess shear stress [N/m²]:

$$\tau_* = \frac{\tau_b - \tau_{cE}}{\tau_{cE}} \quad \tau_b \geq \tau_{cE} \quad \text{Equation 31}$$

$$\tau_* = 0 \quad \tau_b < \tau_{cE} \quad \text{Equation 32}$$

where τ_b is the bottom shear stress [N/m²] and τ_{cE} is the critical shear stress for erosion [N/m²].

The set of cohesive constants can be specified for each solid in the Constants section, Solids Transport group. The shear stress multiplier varies between 0.1 – 100 [g/m²-s], with a default value of 5. The shear stress exponent varies between 1.6 – 4, with a default value of 3. The critical shear stress for erosion varies between 0.5 – 8 [N/m²], with a default value of 2.

The shear stress multiplier, exponent, and the critical shear stress for erosion can vary spatially in a water body. Input different values for these for each surface benthic segment

in the Parameter Data, Solids group. If a nonzero value is specified for a segment, that value is used instead of the constant.

3.7 Biotic Solids Production and Dissolution

Biotic solids include living algae and non-living detritus. The WASP8 eutrophication model simulates the growth, settling and death of phytoplankton and macro algae, with the subsequent production, settling, and dissolution of detritus. The total dry weight of these biotic solids components is added to the inorganic solids concentrations to produce total suspended solids in water column segments.

In the WASP8 toxicant model, one or more solids variables can be characterized as biotic. For solid “i” the net production rate $R_{prod,i}$ [g/m³-d] is given by:

$$R_{prod,i} = (R_{p,seg} + R_{p,t}) \theta_{prod}^{T-20} \quad \text{Equation 33}$$

where $R_{p,seg}$ is the spatially-variable Biotic Solids Net Production Rate [g/m³-d] specified in the Parameters section, Solids group; $R_{p,t}$ is the time-variable Biotic Solids Net Production Rate [g/m³-d] specified in the Time Functions section, and θ_{prod} is the temperature correction coefficient, specified in the Constants section, Solids Transport group.

Similarly, the dissolution rate constant $k_{diss,i}$ [d⁻¹] is given by:

$$k_{diss,i} = (k_{d,seg} + k_{d,t}) \theta_{diss}^{T-20} \quad \text{Equation 34}$$

where $k_{d,seg}$ is the spatially-variable Biotic Solids Dissolution Rate Constant [d⁻¹] specified in the Parameters section, Solids group; $k_{d,t}$ is the time-variable Biotic Solids Dissolution Rate Constant [d⁻¹] specified in the Time Functions section, and θ_{diss} is the temperature correction coefficient, specified in the Constants section, Solids Transport group.

The dissolution rate $R_{diss,i}$ [g/m³-d] is the product of its dissolution rate constant [d⁻¹] and its concentration [g/m³]:

$$R_{diss,i} = k_{diss,i} S_i \quad \text{Equation 35}$$

The inorganic residue of biotic solid “i” dissolution will be added to solid “j” if the user specifies the Ash Dry Weight Residue and the Residue Solid Identification Number in the Constants section, Solids Transport group. The organic carbon fraction of biotic solid “i” dissolution will be added to DOC “k” if the user specifies the Organic Carbon Fraction and Dissolution Product DOC Identification Number in the Constants section, Solids Transport group.

3.8. Solids Burial

Sediments below each water segment can be represented in WASP by using one or more layers. The initial total solids concentration in each benthic segment [mg/L or g/m³] sets its reference bulk density [g/mL] and porosity [L_w/L]. Driven by deposition, erosion (including resuspension and bed load), growth, and dissolution fluxes, WASP8 conducts a solids mass balance in these layers. Two options appear in the Dataset screen – Static (constant volumes) and Dynamic (constant densities). We recommend the Dynamic option

(described below) in which you must also set the benthic time step DT_B in the Dataset screen; the default value is 1 day.

Surface Benthic Layer – The surface benthic layer is active. When solids are deposited, it accumulates volume and depth. When solids are eroded, it loses volume and depth. Except as noted below, the initial reference bulk density and porosity are maintained.

If there are no subsurface benthic layers, deposition causes the surface layer to accumulate depth and volume indefinitely, meaning there is no net burial. Erosion reduces the depth and volume until it reaches 5% of the initial values and no further erosion is allowed.

If there are underlying subsurface benthic layers, the surface layer volume and depth are reset to initial reference values for each benthic time step. The reset correspond to net burial (V_{B1} and d_{B1}) or net erosion (V_{E1} and d_{E1}).

Under depositional conditions, the surface benthic segment buries V_{B1} and d_{B1} to the first subsurface benthic segment at each benthic time step. The solids and pollutant concentrations in the buried volume are also passed downward. The burial velocity, w_{B1} [m/s], from the surface benthic segment is

$$w_{B1} = \frac{d_{B1}}{DT_B} \quad \text{Equation 36}$$

Note that burial velocity is reported in the model output in units of [cm/yr]. The burial fluxes from the surface layer for solids and pollutants are:

$$F_{B1,k} = C_{k,1} w_{B1} \quad \text{Equation 37}$$

where $C_{k,1}$ is the concentration of constituent 'k' in the surface benthic layer [g/m³], and $F_{B1,k}$ is the burial flux [g/m²-s] from the surface benthic layer.

Under erosion conditions, the surface benthic segment recruits V_{E1} and d_{E1} from the first subsurface benthic segment at each benthic time step. The solids and pollutant concentrations in the subsurface volume, $C_{k,B2}$, are also passed 'upward' (the surface benthic segment is moving downward). In subsurface benthic layers, total solids are usually packed more tightly and have higher bulk densities and lower porosities. To preserve mass and volume balance, the surface layer bulk density and porosity are recalculated at each benthic time step. If erosion continues over time, the bulk density and porosity approach the values in the subsurface layer.

Subsurface Benthic Layers – Subsurface benthic layers are passive. Each benthic time step, mass is transported downward or upward through the subsurface layers, depending on whether the surface benthic segment experiences deposition or erosion conditions.

Under deposition, the first subsurface segment receives solids from the surface layer at each benthic time step. If the subsurface segment has a higher bulk density, the buried volume and depth (V_{B1} and d_{B1}) are compressed to V_{B2} and d_{B2} , and pore water is squeezed upward. The compressed

volume V_{B2} is passed downward to the next benthic layer or out of the system. Solids and pollutant concentrations in the subsurface volume, $C_{k,B2}$, are also passed downward to the next lower benthic segment through the bed, maintaining the initial bulk density and porosity.

Under erosion conditions, the surface segment receives volume V_{E1} from the first subsurface layer at each benthic time step. Solids within this volume are also transferred upward. In turn, lower subsurface benthic layers transfer eroded volume and solids concentrations to their overlying benthic layers. Erosion reduces the depth and volume of the bottom layer until it reaches 5% of its initial value; no further erosion of that layer is allowed. Erosion then reduces the depth and volume of the next lowest benthic layer until it, too, reaches 5% of its initial value. If erosion continues, all benthic layers will eventually reach 5% of their initial values. At this point, no more erosion is allowed.

3.9. Analytical Solution for Settling

WASP8 normally uses a backward difference numerical solution technique. For each state variable, the concentration at the beginning of a time step, C_0 , is used in transport and transformation equations. The time step, DT , is adjusted to maintain stability.

For coarse silts and sands, however, high settling velocities could cause WASP8 to use increasingly smaller time steps. When settling removes more than 0.1% of a solid from a water column segment during the normal calculation time step, WASP8 uses the alternative analytical solution, which calculates C^* , the average solid concentration during the time step, applied in the solid settling and advection loss for the time step.

Balancing loading, advection, and settling, the analytical steady-state solution for a solid under prevailing conditions is:

$$C_{SS} = \frac{L}{Q + V \frac{w_s}{d}} \quad \text{Equation 38}$$

where L is the total loading of solid "i" [g/d] including external loadings, advection in, and resuspension; Q is the advective flow [m³/d], V is the segment volume [m³], d is the segment depth [m], and w_s is the settling or deposition velocity [m/d]. During the time step, the concentration will move from C_0 toward C_{SS} .

For convenience, this equation can be rearranged:

$$C_{SS} = \frac{L}{V X_{ks}} \quad \text{Equation 39}$$

where X_{ks} is the overall loss rate constant due to outflow plus settling [1/d]:

$$X_{ks} = \frac{Q}{V} + \frac{w_s}{d} \quad \text{Equation 40}$$

The first order attenuation equation is:

$$\frac{v}{dt} = L - \left(Q + \frac{v w_s}{d} \right) C \quad \text{Equation 41}$$

The solution for C as a function of time is:

$$C = C_0 + \frac{L}{VX_{ks}}(1 - e^{-X_{ks}t}) \quad \text{Equation 42}$$

$$C = C_0 + C_{SS}(1 - e^{-X_{ks}t}) \quad \text{Equation 43}$$

Integrating this equation over DT gives:

$$\int_0^{DT} C dt = \left[-\frac{1}{X_{ks}}(C_0 - C_{SS})e^{-X_{ks}t} + C_{SS}t \right]_0^{DT} \quad \text{Equation 44}$$

evaluating the right-hand side at $t = DT$ minus $t = 0$ and rearranging terms gives:

$$\int_0^{DT} C dt = C_{SS}DT + \frac{1}{X_{ks}}(C_0 - C_{SS})(1 - e^{-X_{ks}DT}) \quad \text{Equation 45}$$

The average concentration during DT is:

$$C^* = \frac{\int_0^{DT} C dt}{DT} = C_{SS} + \frac{1}{X_{ks}DT}(C_0 - C_{SS})(1 - e^{-X_{ks}DT}) \quad \text{Equation 46}$$

It is convenient to define X_{term} , which varies from close to 1 (for small DT or X_{ks}) to 0 (for large DT or X_{ks}):

$$X_{term} = \frac{1 - e^{-X_{ks}DT}}{X_{ks}DT} \quad \text{Equation 47}$$

so that:

$$C^* = C_0X_{term} + C_{SS}(1 - X_{term}) \quad \text{Equation 48}$$

The average concentration C^* varies from C_0 at small time steps or loss rates to C_{SS} for large time steps or loss rates.

3.10. Example

This section describes how interaction of solids behaves between the water column and benthic segments. A simple pond system consisting of a water column, a surface benthic layer, and a subsurface benthic layer model the transport of solids. Table 3 describes the geometry of the segments.

Table 3. Channel Geometry of WASP Segments

Segment	Volume (m ³)	Depth (m)
Water Column	10,000	1
Surface Sediments	200	0.02
Subsurface Sediments	500	0.05

The WASP model simulates flow, as well as silt and sand loads, with simple process-based settling and resuspension. Dynamic bed compaction was used in the sediment layer at a time step of one day. Table 4 describes parameters used and their values.

Table 4. Solids Demonstration Parameters

Variable	Description	Units	Value
Q	Flow through the Water Column	m ³ /d	10,000
S_{silt}	Silt Load into the Water Column	kg/d	60
S_{sand}	Sand Load into the Surface Sediment	kg/d	40
A_{bed}	Cross-sectional Area of Bed	m ²	10,000
r_{silt}	Silt radius	mm	0.004
$v_{s,silt}$	Silt Settling Velocity	m/d	5.E-01
$v_{r,silt}$	Silt Resuspension Velocity	m/d	5.E-05
T_{bed}	Bed Compaction Time Step	d	1

The model is simulated until all three segments have reached steady state, with the subsurface sediment layer taking the longest time. Figures 3-5 show the concentrations of total solids, silt, and sand in each segment layer. Sand is not present in the water column because the load is entered directly into the surface sediment layer. Silt concentrations reach steady state in the water column segment relatively quickly, compared to sediment layers.

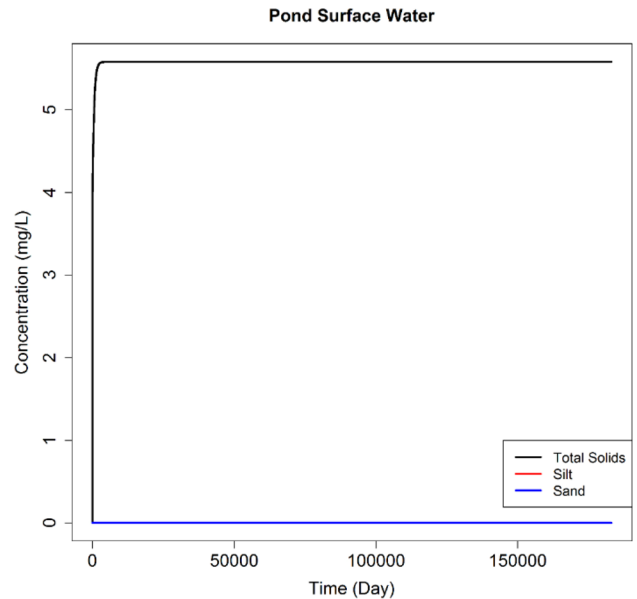


Figure 3. Solids Concentration in the Surface Water

Total solids and sand concentrations are plotted on the left y axis and silt concentrations are plotted on the right. Sand concentration decreases rapidly as silt is deposited from the water column. The dynamic bed compaction option allows the surface benthic layer to accumulate volume and depth until the bed compaction time step is reached, which then resets the volume and depth of the surface benthic segment while burying excess volume and depth to the segment below. Concentration of total solids remains constant after minor volume adjustments in the first few time steps.

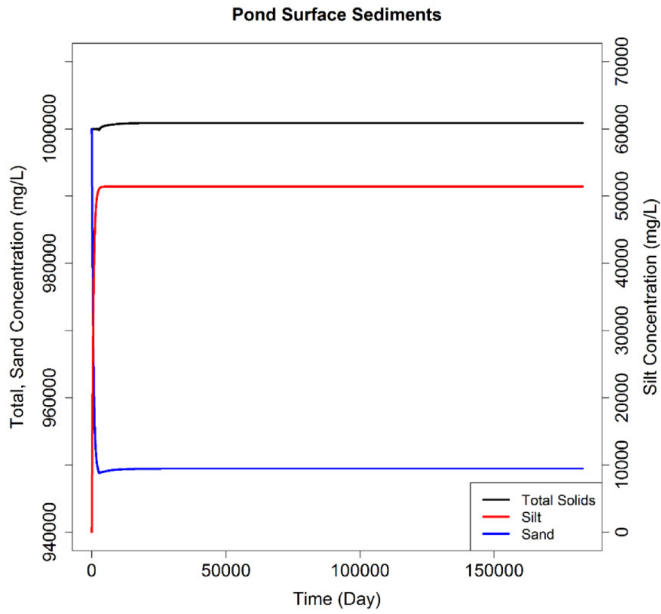


Figure 4. Solids Concentration in the Surface Sediments

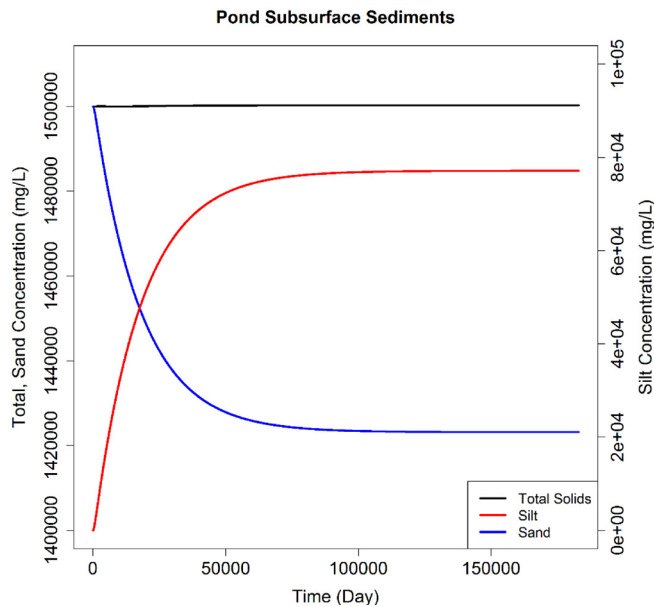


Figure 5. Solids Concentration in the Subsurface Sediments

Sediment composition of the subsurface benthic layer changes more slowly than surface layers as a function of the bed compaction time step. Overall, sand concentration decreases as mass from the surface sediments is buried. Steady state is eventually reached in all three layers. Burial or removal from the subsurface benthic layer is lost from the system and equals the rate of mass being moved downward from the surface benthic layer. Figure 6 shows the burial rates of the surface and subsurface benthic layers.

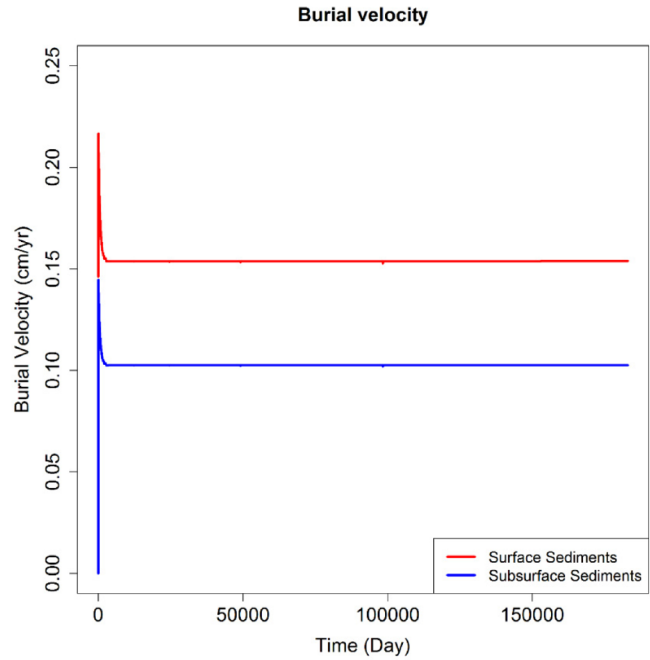


Figure 6. Sediment Burial Rates

4.0 Light

4.1. Introduction

Solar radiation can result in phototransformation of contaminants and constituents in surface water systems. Chemicals, metals, and nanomaterials all undergo photochemical reactions, which can result in the degradation and/or transformation of contaminants. Solar radiation can deactivate pathogens and viruses, and be used for photosynthesis by microorganisms. It is therefore important to capture transmission of light from the water surface and through the water column.

4.2. Theory

Several factors affect the amount of solar radiation within the water column. The amount of light reaching the surface water is affected by clouds and shading of the water, and the amount of radiation is dependent on the time of day and time of year¹¹⁻¹³. Light is comprised of a range of different wavelengths. Total radiation is comprised of different fractions of the different wavelengths. Each wavelength is attenuated as it travels through the water column, and the extent depends on the wavelength as well as factors such as suspended solids and dissolved organic carbon. How WASP addresses light reaching the surface, how it divides up wavelength bands, and how it attenuates light through the water column is detailed in this section.

4.2.1 Light Attenuation

Within the water column, light is attenuated with depth following the Beer-Lambert equation^{14, 15}:

$$I_z = I_0 e^{-K_{e,\lambda} z} \quad \text{Equation 49}$$

where I_z is the light intensity (W/m^2) at depth z , I_0 is the light intensity (W/m^2) at the water surface $K_{e,\lambda}$ is the light extinction coefficient [$1/\text{m}$], λ is the wavelength index, and z is depth below the surface [m].

The light extinction coefficients are calculated internally as a function of background water, algal chlorophyll a, DOC, and solids:

$$K_{e,\lambda} = K_{w,\lambda} + K_{chl,\lambda} (chl)^{a_\lambda} + K_{DOC,\lambda} DOC + K_{TSS,\lambda} TSS \quad \text{Equation 50}$$

where Chl is algal chlorophyll concentration [$\mu\text{g}/\text{L}$], a_λ is a wavelength-specific exponent for chlorophyll, DOC is total dissolved organic carbon [mg/L], TSS is total suspended solids [mg/L], $K_{w,\lambda}$ [$1/\text{m}$] is the light attenuation coefficient of water for wavelength λ , $K_{chl,\lambda}$ [$1/\text{m}$] is the light attenuation coefficient due to chlorophyll for wavelength λ , $K_{DOC,\lambda}$

[$1/\text{m}$] is the light attenuation coefficient due to chlorophyll for wavelength λ , and $K_{TSS,\lambda}$ [$1/\text{m}$] is the light attenuation coefficient due to suspended solids for wavelength λ .

4.3. Implementation

4.3.1 Input Total Radiation

The first aspect of using the light module within WASP8 is to incorporate incident radiation that reaches the surface of the water body. Total solar radiation reaching the water surface can be specified by user input light and internally-calculated diel light. This option is specified in the Constants section, Light group; the default is 0, Calculated diel light.

Option 0, Calculated diel light

Light option 0 is driven by internally-calculated light, based on latitude, longitude, day of year and time of day. The latitude of the water body is input to the Constants section, General group. Simulated day and time are kept internally based on the simulation start day and time and the calculation time step. Calculated light represents clear sky radiation, I_{clear} , in W/m^2 .

Option 1, User Input Diel Light

Light Option 1 is driven by as many as four specified time series of hourly (or less) surface light fluxes. WASP8 assumes that these input functions represent the total spectrum of solar radiation [W/m^2]. At each time step, the model reads the total radiation and applies it to each surface segment.

The appropriate solar radiation time function for each segment (1 – 4) is specified in the Parameter Data section, Environmental group. The solar radiation time functions are entered in the Time Functions section. If the data represent a fraction of the total (i.e., visible or PAR light), or if the data are expressed in alternate units, the user must enter an appropriate scale factor in the “Solar Radiation Multiplier [unitless or W/m^2]” located in the Parameter Data section, Environmental group. To convert from PAR light to total radiation, the multiplier is 2.155.

Option 2, User Input Daily Light, Calculated Diel Light

Total daily light flux – Light Option 2 is driven by as many as four specified time series of total daily surface light fluxes [W/m^2]. On each new simulation day, the model reads the total daily radiation for that day, I_{tot} . At each time step through the diel cycle, the model calculates and applies a portion of the daily total radiation to each surface segment.

The appropriate solar radiation time function for each segment (1 – 4) is specified in the Parameter Data section, Environmental group. The solar radiation time functions are entered in the Time Functions section. If the data are expressed in alternate units, the user must enter an appropriate scale factor in the “Solar Radiation Multiplier [unitless or W/m²]” located in the Parameter Data section, Environmental group.

Default diel light distribution – The default diel cycle is based on latitude, longitude, day of year and time of day. The model calculates the total clear-sky radiation for the day ($I_{ClearDay}$) and the clear-sky radiation for each time step through the day ($I_{ClearSky}$). The instantaneous solar radiation flux is the input total daily flux (I_{Tot}) times the diel ratio for that time step:

$$I = I_{Tot} \left(\frac{I_{ClearSky}}{I_{ClearDay}} \right) \quad \text{Equation 51}$$

The latitude and longitude of the water body is input to the Constants section, General group. The simulation day and time are kept internally based on the simulation start day and time and the calculation time step.

Alternate diel light distribution – An alternative user-controlled diel option is applied if a daylight fraction time function f_{day} is specified. In this case, total daily radiation is distributed through daylight hours (between dawn and dusk) using a half-sine curve with a maximum value at noon.

$$I_{max} = \frac{I_{Tot}\pi}{2f_{day}} \quad \text{Equation 52}$$

$$I = I_{max} \sin(\pi\tau_{day}) \quad \text{Equation 53}$$

where I_{Tot} is the total daily radiation [W/m²], f_{day} is the fraction of day that is daylight (0.2 – 0.8) and τ_{day} is normalized time between sunrise and sunset, expressed as fraction of the daylight interval. Sunrise is 1, noon is 0.5, and sunset is 1. $I = 0$ during nighttime hours.

The “Fraction Daily Light (fraction)” is input to the Time Functions section. The simulation day and time are kept internally based on the simulation start day and time and the calculation time step.

4.3.2. Light Attenuation Above Water Surface

Input solar radiation can be attenuated by cloud cover, canopy shading, ice cover, and water surface reflectance.

Cloud Cover

Internally-generated light (option 1) represents clear sky radiation. This can be attenuated by user-specified cloud cover [fraction of sky].

$$I = 0.65 I_{clear}(1 - Cloud)^2 \quad \text{Equation 54}$$

The appropriate cloud cover time function (1 – 4) is specified for each segment in the Parameter Data section, Environmental group. The cloud cover time functions are entered in the Time Functions section as a fraction (0.0 – 1.0). Options 1 and 2 assume cloud cover is already accounted for in the surface light flux time series.

Canopy Shading

Near-surface light can be diminished by vegetative shading. Light beneath the canopy must be attenuated by user-specified vegetative shading [fraction of light intercepted].

$$I_s = I(1 - Shade) \quad \text{Equation 55}$$

The appropriate canopy shading time function (1 – 4) is specified for each segment in the Parameter Data section, Environmental group. The canopy shading time functions are entered in the Time Functions section as a fraction (0.0 – 1.0).

Water Surface Reflectance

A fraction of light reaching the water surface, I_s , is reflected. Light at the top of the water column, I_o , is reduced by the fraction of light reflected:

$$I_o = I_s(1 - \beta_w) \quad \text{Equation 56}$$

The default reflectance (β_w) is 0.06 and is automatically implemented for surface water segments. The user can input an alternate value in the Constants section, Light group.

Attenuation in Ice

When ice forms on the water surface, the surface light, I_s , is attenuated by reflectance of the ice surface (*albedo*, α), surface absorption (β_i), and light extinction through the ice thickness, h_i .

$$I_o = I_s(1 - \alpha)(1 - \beta_i)e^{-\gamma_i h_i} \quad \text{Equation 57}$$

The default values for albedo, surface absorption, and ice extinction coefficient (γ_i) are 0; these values can be updated in the Constants section, Water temperature group.

Surface ice cover fractions can be input in the Parameter Data section, Environmental group and the Time function group. Together, they give the fraction surface areas covered by ice.

$$F_{ice} = SG_{ice}TF_{ice} \quad \text{Equation 58}$$

Ice thickness is calculated by the temperature module. If water temperature and ice are not being simulated, then the “Minimum ice thickness before ice formation is allowed” is applied as an average thickness. This is input in the Constants section, General group.

4.3.3. Light Attenuation Below the Water Surface

As discussed previously, within the water column, light is attenuated with depth following the Beer-Lambert equation:

$$I_z = I_o e^{-K_{e,l} z} \quad \text{Equation 59}$$

where $K_{e,l}$ is the light extinction coefficient [1/m], l is the wavelength index, and z is depth below the surface [m].

Table 5. WASP Default Light Extinction Coefficients for the Wavelength Bands

Index	Color	Water [m ⁻¹]	Chlorophyll [m ⁻¹ (µg/L) ⁻¹]	DOC [m ⁻¹ (mg/L) ⁻¹]	Solids [m ⁻¹ (mg/L) ⁻¹]
1	UVB med	0.151	0.103	6.22	0.34
2	UVB high	0.109	0.0816	5.40	0.34
3	UVA low	0.0805	0.069	4.59	0.34
4	UVA med	0.0512	0.057	3.40	0.34
5	UVA high	0.0340	0.053	2.54	0.34
6	violet	0.0169	0.039	1.266	0.34
7	blue	0.0166	0.0262	0.514	0.34
8	green	0.0475	0.0143	0.289	0.34
9	yellow-orange	0.217	0.0063	0.115	0.34
10	red	1.007	0.0065	0.0	0.34
11	infrared	2.07	0.0	0.0	0.34

The light extinction coefficients are calculated internally as a function of background water, algal chlorophyll a [µg/L], chlorophyll exponent [unitless], DOC [mg/L], and solids [mg/L]:

$$K_{e,\lambda} = K_{w,\lambda} + K_{chl,\lambda}(chl)^{exp_{\lambda}} + K_{DOC,\lambda}DOC + K_{solid,\lambda}TSS \quad \text{Equation 60}$$

Table 5 provides the default coefficients by wavelength.

The chlorophyll exponent by wavelength defaults to 1. The coefficients for total ultraviolet and total visible light are calculated internally as the weighted sum of their component wavebands (1 – 5 for ultraviolet, 6 – 10 for visible).

The default coefficients for visible light are listed in Table 6. Division of Wavelengths by Wave Class. These can be

Table 6. Division of Wavelengths by Wave Class

Wave Class	Color	Wavelengths, nm	Fraction of Total
1	ultraviolet	295 – 379	0.036
2	visible	380 – 749	0.464
3	infrared	750 – 2500	0.500

Table 7. Division of Wavelengths into Wave Bands, with Fractions Given by Latitude

Index	Color	Wavelengths [nm]	Latitude						
			0° N	10° N	20° N	30° N	40° N	50° N	60° N
1	UVB med	295 – 304	0.00015	0.00015	0.00013	0.00011	0.00008	0.00006	0.00004
2	UVB high	305 – 314	0.00142	0.00139	0.00132	0.00120	0.00104	0.00085	0.00067
3	UVA low	315 – 334	0.00845	0.00839	0.00825	0.00801	0.00766	0.00721	0.00681
4	UVA med	335 – 354	0.01141	0.01137	0.01126	0.01108	0.01082	0.01052	0.01054
5	UVA high	355 – 379	0.01723	0.01718	0.01706	0.01686	0.01655	0.01619	0.01630
6	violet	380 – 449	0.07626	0.07617	0.07593	0.07550	0.07482	0.07394	0.07443
7	blue	450 – 494	0.06664	0.06663	0.06659	0.06652	0.06639	0.06616	0.06644
8	green	495 – 569	0.10386	0.10388	0.10394	0.10402	0.10406	0.10390	0.10285
9	yellow-orange	570 – 619	0.06546	0.06549	0.06556	0.06566	0.06576	0.06568	0.06422
10	red	620 – 749	0.14914	0.14934	0.14995	0.15106	0.15282	0.15550	0.15769

changed in the Constants group, Light section. If multiple fractions of DOC are simulated, the user can enter a set of light extinction coefficients for each DOC fraction.

Total solar radiation is divided into three classes:

The classes are used in the heat balance equations in the WASP8 Temperature module, and in the bacterial death equations.

Table 7 provides how WASP divides ultraviolet and visible solar radiation into 10 wave bands.

These wavebands allow each band to have its own light attenuation as it penetrates the water column. The radiation of each wavelength band then drives photochemical reactions.

WASP8 uses time series of total radiation, along with waveband fractions, to deliver solar radiation to the water surface. The total radiation can be input by the user or calculated internally by the model. Waveband fractions can be specified or default values used.

5.0 Particle Attachment

5.1. Introduction

Sorption is the association of aqueous species with a solid material¹⁶. Surface waters are abundant with suspended solids (e.g., silt, clay and particulate organic matter), and sorption affects the fate transport of contaminants in surface waters. Sorption involves sorption and desorption^{17, 18}.

Sorption is the association of a contaminant with the surface of a solid particle. Desorption is the reverse and describes dissociation of a sorbed molecule and its return to the aqueous or gaseous phase.

Depending on system assumptions, sorption can be simulated by an equilibrium or kinetic model. If an equilibrium model is used, it is assumed that sorption is fast and occurs instantaneously. If a kinetic model is used, the processes are simulated as two competing reactions.

Previous versions of WASP included equilibrium sorption only, but WASP8 includes kinetic sorption, as well as heteroaggregation of nanomaterials.

5.2. Theory

5.2.1. Equilibrium Sorption

Sorption reactions are usually fast, relative to environmental processes, and equilibrium may be assumed. For environmentally relevant concentrations (less than 10⁻⁵ M or one-half water solubility), equilibrium sorption is linear with dissolved chemical concentration¹⁹ or:

$$C_i^S = K_{d,i} C_i^W \quad \text{Equation 61}$$

where C_i^S is chemical concentration in the solid phase and C_i^W is chemical concentration in the aqueous phase. Table 8 provides a full list of parameter descriptions used in this section.

Table 8. Equilibrium Sorption Parameters

Symbol	Definition	Units
C_i	Total Chemical i Concentration	mg _{chem} /L
C_i^W	Dissolved Chemical i Concentration	mg _{chem} /L
C_i^W	Dissolved Chemical i Concentration in Water $C_i^W = C_i^W/n$	mg _{chem} /L _w
$C_i^S_j$	Concentration of Sorbed Chemical i on Solid j	mg _{chem} /L
$C_i^S_j$	Concentration of Sorbed Chemical i on Solid j $C_i^S_j = C_i^S_j/S_j$	mg _{chem} /kg _s

Symbol	Definition	Units
s_j	Solid j Concentration	mg _s /L
S_j	Solid j Concentration $S = s \times 10^{-6}$	kg _s /L
S_j^W	Solid j Concentration in Water	kg _s /L _w
n	Porosity or Volume Water per Volume	L _w /L
$K_{d,i,j}$	Partition Coefficient of Chemical i on Solid j	L _w /kg _s
$f_{d,i}$	Fraction of Chemical i in Dissolved Phase	-
$f_{s,ij}$	Fraction of Chemical i Sorbed to Solid j	-

At equilibrium, distribution between the aqueous phase and the solid phase is determined by partition coefficients. When multiple solid phases are present (e.g., sand, silt, clay, organic matter), the total mass of chemical associated with each phase is controlled by $K_{d,i,j}$, where i represents the specific chemical and j is the solid phase of interest (e.g. $K_{d,i \text{ sand}}$, $K_{d,i \text{ silt}}$, $K_{d,i \text{ clay}}$, and $K_{d,i \text{ organic}}$). Complexation with DOC is handled in a similar manner, using the same equations and associated $K_{d,i \text{ DOC}}$. All of these relationships are solved simultaneously, assuming instantaneous distribution among the phases (equilibrium assumption). The fraction of mass associated with each phase is given by:

$$f_{d,i} = \frac{n}{n + \sum_{j=1}^n K_{d,i,j} S_j} \quad \text{Equation 62}$$

and

$$f_{s,ij} = \frac{K_{d,i,j} S_j}{n + \sum_{j=1}^n K_{d,i,j} S_j} \quad \text{Equation 63}$$

where $f_{d,i}$ is the fraction of chemical i concentration present in the freely dissolved form, $f_{s,ij}$ is the fraction of chemical i sorbed to solid j . If complexation with DOC is simulated, the fraction in the aqueous phase includes the freely dissolved form and all complexed with DOC. These functions are determined in time and space throughout a simulation from the partition coefficients, internally calculated porosities, and simulated sediment concentrations.

In addition to the assumption of instantaneous equilibrium, the assumption of reversibility is also implicit in the use of these equations. Laboratory data for very hydrophobic chemicals suggest, however, that a hysteresis exists, with desorption being much slower than adsorption. They also suggest this effect may be the result of intraparticle kinetics in which the chemical is slowly incorporated into components of the sorbant.¹⁹

Site-specific values for partition coefficients can be obtained from laboratory experiments or field data; literature values may be used in lieu of site-specific values. WASP can also simulate equilibrium partitioning to DOC state variables, but is not included in current documentation. A more comprehensive discussion of chemical processes will be released in the WASP8 manual.

5.2.2. Kinetic Sorption

When the equilibrium assumption is not applicable, sorption can be simulated kinetically which incorporates a forward reaction and competing reverse reaction. Because the system is changing dynamically, separate state variables must be incorporated to represent freely-dissolved chemical, $Chem_1$ (mg/L), and chemical sorbed to the solid particles, $Chem_2$ (mg/L). The sorption process is described by the following differential equation:

$$\frac{d[Chem_1]}{dt} = -k_{for}[Chem_1][S] + k_{rev}[Chem_2] \quad \text{Equation 64}$$

where $[S]$ is the suspend solid concentration in the aqueous phase (mg/L), k_{for} is the forward, sorption rate constant (L/mg-d), and k_{rev} is the reverse, desorption rate constant (1/d).

$[Chem_2]$ is the contaminant concentration sorbed on the solid, which can be expressed as:

$$[Chem_2] = [Chem_1]_0 - [Chem_1] \quad \text{Equation 65}$$

where $[Chem_1]_0$ represents the initial contaminant concentration (mg/L) in surface waters.

Therefore, Equation 1 can be derived into the following differential equation:

$$\frac{d[Chem_1]}{dt} = -k_{for}[Chem_1][S] + k_{rev}([Chem_0] - [Chem_1]) \quad \text{Equation 66}$$

Initial contaminant concentration ($CHEM_0$) and initial solid concentration (S_0) are set in the Segment section, Initial Conditions group.

5.2.3. Nanomaterial Heteroaggregation

The architecture of the WASP has been redesigned to allow simulation of nanomaterials.

A new state variable class NANOC, for nanomaterials, is included in WASP8 which uses the kinetic process of heteroaggregation^{20,21} to simulate attachment of a nanomaterial to suspended particulate matter. Heteroaggregation is the process by which nanoparticles collide and stick to particulate matter, based on three separate collision processes. The overall heteroaggregation rate is defined by:

$$k_{het,ij} = \alpha k_{coll,ij} N_j^{SPM} \quad \text{Equation 67}$$

where

α : The collision efficiency or the probability that a nanoparticle will stick to a suspended solid particle in the event of a collision. This is a unitless parameter that can range between 0-1.

$k_{coll,ij}$: The rate of collision between two particles in units of volume per day.

N_j^{SPM} : The number of suspended particulate matter per volume.

$k_{coll,ij}$ is defined by:

$$k_{coll,ij} = \frac{2k_B T_{water} (r_{NP,i} + r_{SPM,j})^2}{3\mu_{water} r_{NP,i} r_{SPM,j}} + \frac{4}{3} G (r_{NP,i} + r_{SPM,j})^3 + \pi (r_{NP,i} + r_{SPM,j})^2 |v_{set,i}^{NP} - v_{set,j}^{SPM}| \quad \text{Equation 68}$$

which consists of three components:

$$\text{Brownian Motion} = \frac{2k_B T_{water} (r_{NP,i} + r_{SPM,j})^2}{3\mu_{water} r_{NP,i} r_{SPM,j}} \quad \text{Equation 30a}$$

$$\text{Fluid Motion} = \frac{4}{3} G (r_{NP,i} + r_{SPM,j})^3 \quad \text{Equation 30b}$$

$$\text{Differential Settling} = \pi (r_{NP,i} + r_{SPM,j})^2 |v_{set,i}^{NP} - v_{set,j}^{SPM}| \quad \text{Equation 30c}$$

Parameter descriptions and values used in this analysis are presented in Table 31. The rate of collision between nanoparticles and particulate matter is dependent on three processes: Brownian motion (perikinetic aggregation), fluid motion (orthokinetic aggregation), and differential settling. Settling velocity is calculated using Stokes' law:

$$v_{set}^{particle} = \frac{2}{9} g \frac{(\rho_{particle} - \rho_{water}) r_{particle}^2}{\mu_{water}} \quad \text{Equation 69}$$

Assuming a spherical particle, is calculated by:

$$N_j^{SPM} = \frac{S_j^{SPM}}{\rho_{SPM,j} \frac{4}{3} \pi r_{SPM,j}^3} \quad \text{Equation 70}$$

The heteroaggregation process is described by the following differential equation:

$$\frac{\Delta C N_i^{WC}}{\Delta t} = -k_{het} N_i^{WC} S_j \quad \text{Equation 71}$$

The collision efficiency is a system dependent parameter that must be measured or estimated. is calculated internally by WASP. These equations assume that the particles collide with nanoparticles at the same rate as hard spheres.

5.3. Implementation

In the Constant Group section, Chemical Kinetic Sorption group, reaction products must be specified to simulate contaminant transport. This is implemented by checking the 'Chemical sorbed to Solid (i), [ID#]' for the desired chemical (ID#) and solid (i) state variables, and entering a value pointing to the sorbed chemical.

5.3.1. Equilibrium Sorption

To assign a partition coefficient of a dissolved chemical to a solid, check the 'Partition Coefficient of chemical to Solid(1), [L/kg], CHEM1' constant and enter a coefficient in the

value column. Unlike kinetic sorption and heteroaggregation which handle phases as different state variables, equilibrium sorption uses initial total concentration of a single state variable to partition dissolved and sorbed chemical concentrations internally in WASP8, and outputs them as different time series.

5.3.2. Kinetic Sorption

To assign sorption (k_{for}) and desorption (k_{rev}) rates to a chemical, check the 'Sorption rate constant to Solid (1), [L/kg-d], CHEM1,' and 'Desorption rate constant from Solid (1), [1/d], CHEM2,' and enter rates in the value column.

5.3.3. Nanomaterial Heteroaggregation

In the Systems section, users can add nano chemical (NANOC) state variables to the model with unique names and densities. Users must add a nano state variable for each phase of a specific nano chemical *i* (e.g., aqueous phase, sorbed phase to solid *j*, etc.). Nano state variables that represent heteroaggregated phases assume the density, diameter, and settling rate of the solid that it is sorbed to. Concentrations can be added to the system as initial conditions (IC) in the Segments section, Initial Conditions tab, or as boundary

conditions (BC) in the Boundaries and Loads section. IC and BC are entered as mg/L. Loads are entered as kg/d.

Under the Parameter Data Group section, Nano Chemical group, nano chemical collision efficiency (α) and nano chemical settling velocity can be entered for each segment. Input values will only display the first four decimal places, but WASP8 retains the value even if it is too small to display. For small values, the Scale Factor ensures that the entered values can be seen.

Under the Constant Group section, Nano Chemical Kinetic Sorption group, reaction products must be specified to simulate contaminant transport. This is implemented by checking the 'Nano chemical sorbed to Solid (*i*), [ID#]' for the desired nanochemical (ID#) and solid (*i*) state variables, and entering a value pointing to the sorbed nano chemical. Particle diameter,s which are used in the heteroaggregation equation, must be specified in the Nano Chemical Partitioning group.

6.0 Nanomaterial Reactions

6.1. Introduction

Nanomaterials are routinely defined as materials sized between 1 nm to 100 nm, with properties not found in bulk samples of the same materials.²²⁻²⁴ Engineered nanomaterials (ENMs) have been applied in all areas of our daily lives, and their production has increased appreciably in recent years.²⁵⁻³¹ Such rapid expansion of ENM production increases the likelihood of ENPs being released into the environment. Besides the heteroaggregation process in surface waters, ENMs may undergo transformation reactions including photochemically-driven reactions, sulfidation, oxidation, and dissolution. For example, graphene oxide undergoes phototransformation under simulated sunlight radiation, resulting in reduced graphene oxide and polycyclic aromatic hydrocarbons (PAHs).^{32, 33} Dissolution,³⁴⁻³⁶ oxidation^{37, 38} and sulfidation^{34, 39-41} are common reactions to metal nanomaterials.

To simulate the fate of nanomaterials in aquatic environments, WASP8 incorporates algorithms to describe ENM reactions. WASP8's Advanced Toxicant Module simulates 10 state variables for nanomaterials and dissolved chemicals, respectively. This limit can be adjusted upward to handle any number of state variables. WASP8 users may simulate concentrations of multiple nanomaterials, their heteroaggregated forms, and their reaction products in surface waters and sediments. Nanomaterials are simulated using the WASP nanomaterial state variables; dissolved chemicals (e.g., organics, metal ions) are simulated using chemical state variables. For internal calculations, WASP8 assumes a spherical shape for nanomaterials. Another assumption is that a nanomaterial keeps uniform size and morphology both before and after reactions.

Figure 7 Possible Nanomaterial Reaction Pathways. Chem indicates dissolved chemicals (e.g., organics, metal ion) shows different possible reaction pathways for nanomaterials and chemicals.

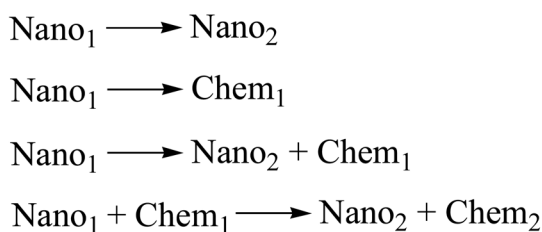


Figure 7 Possible Nanomaterial Reaction Pathways. Chem indicates dissolved chemicals (e.g., organics, metal ion)

6.2. Nanomaterial Reactions

6.2.1. General Reactions Module

The WASP8 nanomaterial reaction module employs a general reaction to simulate nanomaterial reactions which consider a series of factors. The general form reaction rate constant in WASP8 is structured as

$$k_{reaction} = k_{rate} X_{temp} X_{phase} X_{seg} X_{conc} X_{env} \quad \text{Equation 72}$$

where $k_{reaction}$ is the overall reaction rate constant (d^{-1}), k_{rate} is the base reaction rate constant (d^{-1}) at 20°C, X_{temp} is the temperature correction factor, X_{phase} is the phase multiplication factor, X_{seg} is the segment type multiplication factor, X_{conc} is the Monod Equation term, and X_{env} is the environmental factor structured similarly to Monod kinetics.

k_{rate} is the first-order reaction rate constant at 20°C that is input into WASP8. The other terms default to 1 in Equation 72 if no other terms are entered. The default reaction for nanomaterial follows first-order kinetics. If the reaction rate is influenced by other terms or WASP8 users intend to simulate second-order reaction, users turn on the other terms and input their values.

Nanomaterial reactions are essentially surface area-dependent, because only nanomaterial surfaces are available. The first-order nanomaterial surface reaction is expressed as

$$\frac{dm_{NP}}{dt} = -k_{SA} A_{NP} \quad \text{Equation 73}$$

where m_{NP} is the mass of nanomaterials (μg), k_{SA} is the surface-area-normalized reaction rate ($\mu\text{g}/\text{m}^2\text{-d}$), and A_{NP} is the total surface area of nanomaterials (m^2).

Because a key assumption in WASP8 is a nanomaterial keeps uniform size during the reaction, A_{NP} is

$$A_{NP} = \frac{m_{NP}}{\rho_{NP} V_{NP}} (4\pi r^2) = \frac{m_{NP}}{\rho_{NP} (\frac{4}{3}\pi r^3)} (4\pi r^2) \quad \text{Equation 74}$$

where ρ_{NP} is nanomaterial density (g/m^3), V_{NP} is the volume of a single nanoparticle (m^3), m_{NP} is the total quantity of nanomaterials, and r is the radius of a single nanoparticle (m), assuming a spherical structure.

The nanomaterial surface area-dependent reaction can be written as

$$\frac{dm_{NP}}{dt} = -k_{SA} \frac{m_{NP}}{\rho_{NP} (\frac{4}{3}\pi r^3)} (4\pi r^2) = -k_{SA} \frac{3m_{NP}}{\rho_{NP} r} = -\left(\frac{3k_{SA}}{\rho_{NP} r}\right) m_{NP} = -km_{NP} \quad \text{Equation 75}$$

where k is first-order reaction rate constant (d^{-1}).

Since we assume nanomaterial size remains uniform during reactions, we use a mass-dependent reaction. Another reason

is that when users create a nanomaterial state variable in WASP, it is convenient to input nanomaterial mass (or concentration) rather than nanomaterial surface area.

6.2.2. Effect of Temperature

The temperature corrector factor must be turned on in WASP8 to capture the effect of temperature. The van't Hoff-Arrhenius relationship adjusts the value of the reaction rate constant to reflect the effect of temperature:

$$X_{temp} = \theta^{(T-20)} \quad \text{Equation 76}$$

where θ is the temperature-activity coefficient, and T is temperature ($^{\circ}\text{C}$). θ value can be set in WASP8, based on different reaction types.⁴² For example, typical values for θ vary from 1.020 - 1.10 for a biodegradation reaction.

6.2.3. Phase Multiplication Factor

X_{phase} is the phase multiplication factor used to account for processes happening in different phases. For example, if a certain nanomaterial is sorbed on a solid, or the surface is coated with DOC, the physicochemical properties might differ from pristine nanomaterial, and reaction rate might change. Also, if silver nanoparticle (AgNP) surface is associated with DOC in surface waters, the AgNP dissolution rate may be reduced.

Phase multiplication factor is expressed as

$$X_{phase} = f_{nano}x_{nano} + f_{doc}x_{doc} + f_{solid}x_{solid} \quad \text{Equation 77}$$

where f_{nano} , f_{doc} , and f_{solid} are the mass fractions of nanomaterial in its pristine form, nanomaterial coated with DOC, and nanomaterial sorbed on solid phase, respectively. Their relationship is

$$f_{nano} + f_{doc} + f_{solid} = 1 \quad \text{Equation 78}$$

x_{nano} , x_{doc} , and x_{solid} are phase multiplication factor for its pristine form, nanomaterial complexed with DOC, and nanomaterial sorbed on solid phase. The default values for each of these three rate multipliers is 1. The use of f_{solid} is specifically for sorbed nanomaterials. When a nanomaterial heteroaggregates with a solid phase, it is accounted for by using a separate state variable, and all reactions are structured for that variable.

6.2.4. Segment Multiplication Factor

Like most pollutant fate models for surface waters, WASP8 breaks the modeled region into different segments along the river mainstream. Reaction rates for nanomaterial or dissolved chemicals may be different in different segments, and WASP8 users can adjust reaction rates in different segments by using the segment multiplication factor option. Segment multiplication factors include water column (x_{wc}), surface sediment (x_{s1}), and subsurface sediment (x_{s2}).

An example would be a river divided into five segments along the mainstream, where AgNPs are released in the first segment and dissolution rates for AgNPs in these five segments are 0.0010, 0.0013, 0.0006, 0.03, and 0.00058 d^{-1} , respectively, in the water column. In WASP8, users can

set a dissolution rate in "Constant Group," and use a phase multiplication factor to adjust dissolution rates in different segments. For this example, users set a dissolution rate as 0.0010 in "Constant Group" for water column and segment multiplication factors from segments 1 - 5 as 1, 1.3, 0.6, 30, and 0.58, respectively.

If users want different reaction rates in the sediment in different segments, they can follow the approach described above.

6.2.5. Monod Kinetics

X_{conc} is the factor that accounts for Monod-type kinetics as a function of the nanomaterial structure. This is structured in WASP as follows

$$X_{conc} = \frac{K_m}{K_m + Nano} \quad \text{Equation 79}$$

where K_m is the Monod half-saturation coefficient (mg/L). This is structured so that the base reaction rate constant, k_{rate} , must be adjusted so the maximum reaction rate is .

6.2.6. Environmental Kinetics

Similar to Monod kinetics, environmental factors can be incorporated into the reaction rate using X_{env} . This can incorporate oxidation with oxygen, for example. This is structured in WASP as

$$X_{env} = \frac{E_x}{K_e + E_x} \quad \text{Equation 80}$$

where E_x is the environmental concentration of interest (mg/L) (e.g., oxygen, sulfate) and K_e is the half-saturation coefficient for this environmental parameter. The use of this functionality requires an E-option switch of 1, 2, or 3. If the switch is 1, then $X_{env} = 1$. If the switch is 2, then it is modeled as second order and $X_{env} = E_x$. If the switch is 3, Equation 81 is used.

6.3. Nanomaterial Phototransformation

Nanomaterials can undergo phototransformation. For example, lab studies show graphene oxide (GO) undergoes phototransformation under simulated sunlight radiation, resulting in products that include reduced GO (rGO) and polycyclic aromatic hydrocarbons (PAHs). Nanomaterial phototransformation follows first-order kinetic reaction as:

$$\frac{dN}{dt} = -k_{photo}N \quad \text{Equation 81}$$

where k_{photo} is the phototransformation rate constant (d^{-1}), and N is nanomaterial concentration (ng/L).

Formations of new nanomaterials and dissolved chemicals can be simulated using first-order kinetics. The reaction yield coefficient (g/g) in WASP8 allocates how much of each daughter product (nanomaterials and dissolved chemicals) is formed.

In WASP8, the spectrum of sunlight is divided into 11 specific wavelength bands, as shown in Tables 3-5. The division is owing to the fact that different wavelengths drive different environmental processes.⁴³⁻⁴⁸ Since infrared light is generally not photoreactive, we only consider contributions

of ultraviolet and visible lights to the phototransformation rate constants. WASP8 calculates the phototransformation rate constant for each wavelength first, then lumps these 10 together. The lumped photoreaction rate constant is expressed as:

$$k_{photo} = \sum_{\lambda=1}^{10} (k_{photo,\lambda}) \quad \text{Equation 82}$$

where k_{photo} is the overall phototransformation rate constant (d^{-1}) and $k_{photo,\lambda}$ is the phototransformation rate constant (d^{-1}) for each specific wavelength, λ . An example is available to show how to calculate k_{photo} in WASP8.

6.4. Implementation

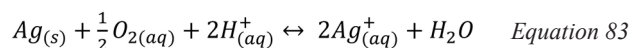
First-order kinetic rate constants and other correctors can be set in the Nano Chemical Photolysis and Nano Chemical Decay sections. Besides setting the wavelength-dependent reaction rate constant for Nano Chemical Photolysis, the solar radiation intensity data should use WASP's light routines.

6.5. Examples

6.5.1. Silver Nanoparticles Dissolution

Silver nanoparticles (AgNPs) are one of the most widely used nanomaterials. AgNPs dissolution is the heterogeneous reaction of AgNPs surface with oxygen in aquatic environments, and AgNPs dissolution is a size-controlled process. Most studies suggest that solubility of AgNPs increases as their size decreases.⁴⁹⁻⁵¹

Several studies simulate silver ion release using first-order reaction kinetics, with the model fitting well with experimental data.⁵²⁻⁵⁴ Peretyazhko et al. studied size-controlled dissolution of AgNPs at neutral and acidic pH conditions. They found that AgNPs increase in size after dissolution, which follows first-order reaction kinetics.⁵⁴ Zhang et al. indicate that dissolved oxygen (DO) significantly influences AgNPs aggregation kinetics, and that aggregation rate increases when DO is present compared to those without DO.⁵⁵ DO and proton concentrations can affect silver ion dissolution kinetics based on the heterogeneous reaction that occurs on AgNPs surfaces in the aquatic environment:



The consumption of $[O_2]$ and $[H^+]$ from AgNPs in the aquatic environment is negligible.⁵³ Besides first-order reaction, Martin, et al. found that silver ion release matches second-order kinetics for protein-coated AgNPs.⁵⁶

WASP8 can simulate first-order and second-order kinetic reactions. We also assume that the nanomaterial maintains a uniform size throughout the reaction process. It has been suggested that even though nanomaterial size changes after reaction, reaction can still match first-order or second-order reaction kinetics.

Here, we demonstrate the simulation of AgNP dissolution. Experimental dissolution data are obtained from Zhang et al.'s publication.⁵³ In WASP8, AgNPs are simulated using the nanomaterial state variable, and dissolved silver ion as a chemical state variable. Dissolution rate is set in "Constant

Group" "Nanodecay" section. Parameters like nanomaterial density and diameter can be set in the "System" and "Constant Group." Heteroaggregation coefficient can be set in "Parameter."

The equation used to model AgNPs dissolution derived in Zhang et al.'s publication can be simplified as:

$$[Ag^+]_{released} = [Ag]_{initial} [1 - \exp(-at)] \quad \text{Equation 84}$$

where $[Ag^+]_{released}$ is the aqueous silver ion ($\mu g/L$), $[Ag]_{initial}$ is the fitted initial aqueous AgNP concentration ($\mu g/L$), and a is dissolution rate constant (h^{-1}). Experimental data indicated that

$$[Ag]_{total} = [Ag^+]_{released} + [Ag] \quad \text{Equation 85}$$

where $[Ag]$ is AgNP concentration at a given time ($\mu g/L$), and $[Ag]_{total}$ is the sum of $[Ag]$ and $[Ag^+]_{released}$ concentrations when t is zero.

We choose two sets of data from Zhang et al.'s publication.⁵³ The first data set for AgNP dissolution kinetics is that size of AgNPs is 40 nm, $[Ag]_{total}$ is 300 $\mu g/L$. The second has AgNP size of 80 nm and $[Ag]_{total}$ is 600 $\mu g/L$. Two types of AgNPs in WASP8 are created as two nanomaterial state variables, and two chemical state variables are created that correspond to dissolved silver ion released from each type. First-order reaction kinetics simulate $[Ag^+]_{released}$ and $[Ag]$ in aqueous solution. The reaction rate constant and $[Ag]_{initial}$ are available in Zhang et al.'s publication.

Data retrieved from Zhang et al.'s paper and WASP simulated results are presented in Table 9. Figure 8 shows experimental data and WASP8 simulation results. Simulation results are similar to Zhang et al.'s publication: for the first eight hours, results show that overall R2 values for 40 nm-300 $\mu g/L$ and 80 nm – 600 $\mu g/L$ are 0.98 and 0.99, respectively; between 8 – 96 hours, R2 values are 0.97 and 0.95, respectively. R2 values are lower between 96 – 300 hour -- 0.71 and 0.62, respectively -- possibly due to aggregation effects.

In Peretyazhko et al.'s paper,⁵⁴ the following equation is used to model $[Ag^+]_{released}$ in aqueous solution:

$$[Ag^+]_{released} = [Ag^+]_{total} [1 - \exp(-kt)] \quad \text{Equation 86}$$

where $[Ag^+]_{released}$ is silver ion concentration in aqueous solution at a given time, and $[Ag^+]_{total}$ is total dissolved silver concentration when no further silver ion concentration increases in aqueous solution during the reaction, and k is dissolution rate. Their research also gets satisfactory agreement between experimental data and model fitting. Because they didn't provide experimental data, we made no effort to fit it, however, the example shows that WASP8 is able to simulate first-order and second-order dissolution reactions.

Besides AgNPs dissolution, new updates of WASP8 can simulate the fate of AgNP in surface waters, which are summarized in Dale et al.⁵⁷

Table 9. Data retrieved from publication and WASP8 simulated results

Time (hour)	40 nm - 300 uL/L		80 nm - 600 uL AgNPs	
	Dissolved silver ion data from Zhang et al's paper	Dissolved silver ion simulated by WASP8	Dissolved silver ion data from Zhang et al's paper	Dissolved silver ion simulated by WASP8
0	12	0.00	12	0.00
2	18	6.41	12	4.18
4	21	12.16	12	7.97
8	27	21.96	18	14.53
12	30	29.84	18	19.93
24	39	45.42	30	31.04
48	51	57.78	36	40.69
72	54	61.15	42	43.69
96	60	62.07	48	44.62
144	63	62.39	48	45.00
192	66	62.41	48	45.03
240	66	62.41	42	45.04
288	69	62.41	48	45.04
336	63	62.41	48	45.04

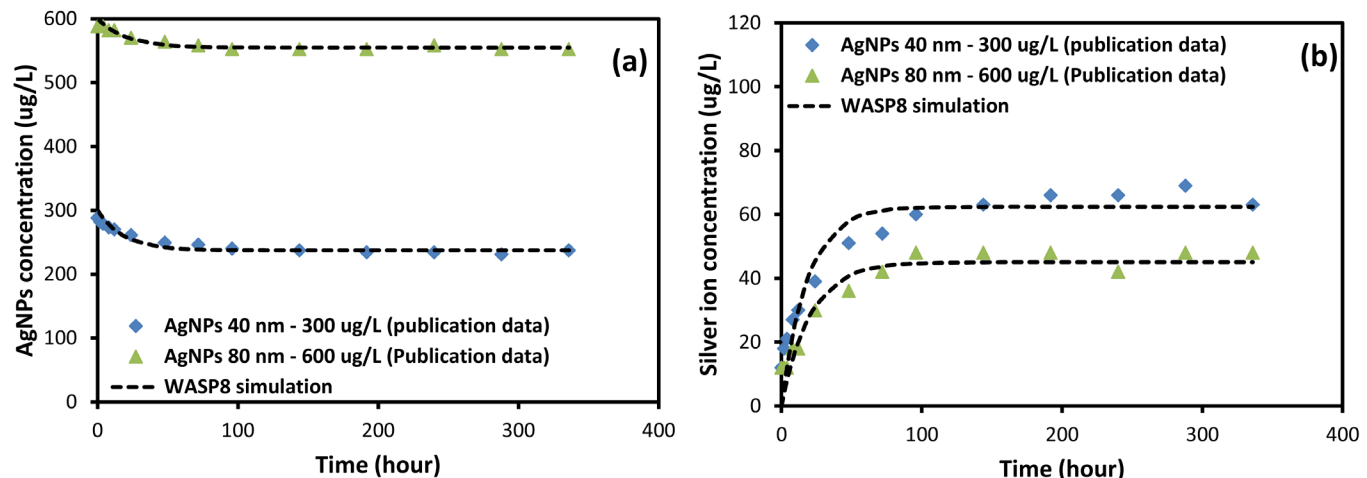


Figure 8. (a) [Ag] experimental data and WASP8 simulation results, (b) [Ag⁺]_{released} experimental data and WASP8 simulation results.

6.5.2. Calculation of Nanomaterial Phototransformation Rate Constants

This example shows how WASP8 internally calculates nanomaterial phototransformation rate constants. WASP8 divides the light spectrum into 10 specific wavelengths. The wavelength-dependent reaction rate constant k_{obs}^n / I^n ($d^{-1}m^2/W$) is determined. k_{obs}^n (d^{-1}) is the reaction rate constant due to the irradiation intensity of I^n (W/m^2), which is the light intensity of a specific wavelength band. Example wavelength-dependent reaction rate constants and wavelength-dependent reaction rates are listed in Table 10.

With the wavelength-dependent reaction rate concentrations determined, the phototransformation rate constant for each wavelength band is calculated as follows:

$$k_{obs,\lambda} = \frac{k_{obs}^n}{I^n} I_{av,\lambda} \quad \text{Equation 87}$$

Table 10. Wavelength-dependent reaction rate of each wavelength band

Wavelength	($d^{-1} (W/m^2)^{-1}$)
620 - 749 nm	0.0001
570 - 619 nm	0.0001
495 - 569 nm	0.0001
450 - 494 nm	0.0001
380 - 449 nm	0.0002
355 - 379 nm	0.0002
335 - 354 nm	0.0002
315 - 334 nm	0.0004
305 - 314 nm	0.0003
295 - 304 nm	0.0003

where $I_{av,\lambda}$ (W/m^2) is average light intensity in water column, and $k_{obs,\lambda}$ (d^{-1}) is the phototransformation rate constant of each wavelength band.

The overall phototransformation rate constant is expressed as

$$k_{obs,overall} = \sum_{\lambda=1}^{10} k_{obs,\lambda} \quad \text{Equation 88}$$

$I_{av,\lambda}$ is average light intensity in water column, which WASP8 calculates by attenuating the sunlight radiation intensity at water surface (I_0). Calculation of average light intensity and light attenuation is documented in Chapter 4. Hourly sunlight intensity on earth surface data in the U.S. can be retrieved from the North American Land Data Assimilation Systems (NLDA5) database. Surface solar radiation varies over the course of the day. Time varying solar radiation data (e.g., hourly) can be input using “Time Functions.” WASP8 can internally calculate the hourly GO phototransformation rate and nanomaterial phototransformation and new nanomaterial production.

6.5.3. Nanomaterial Parallel Reaction

The nanomaterial, graphene oxide, undergoes phototransformation and generates daughter products: reduced graphene oxide and PAHs. This is a parallel reaction whose reaction pathways are shown in Figure 9.

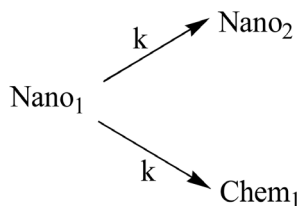


Figure 9. Nanomaterial parallel reaction pathways.

For illustration, we assumed that initial $Nano_1$ concentration is $10 \mu g/L$ and the overall phototransformation rate constant is $0.1 d^{-1}$. Because $Nano_2$ and $Chem_1$ are generated simultaneously, reaction yield (g/g) is introduced to quantify how much of each product is generated. In this example, reaction yield for $Nano_2$ production is $0.9 (Y_1)$, and reaction yield for $Chem_1$ production is $0.1(Y_2)$.

Based on the reaction scheme, reaction rates can be written as:

$$\frac{d[Nano_1]}{dt} = -k[Nano_1] \quad \text{Equation 89}$$

$$\frac{d[Nano_2]}{dt} = -Y_1 k[Nano_1] \quad \text{Equation 90}$$

$$\frac{d[Chem_1]}{dt} = -Y_2 k[Nano_1] \quad \text{Equation 91}$$

WASP8 simulation results are presented in Figure 10. This example shows that WASP8 tracks the degradation of the parent nanomaterial and formation of reaction products.

6.5.4. Segment Multiplication Factor

When conditions change along the course of a water body, it may be useful to incorporate different reaction rates through

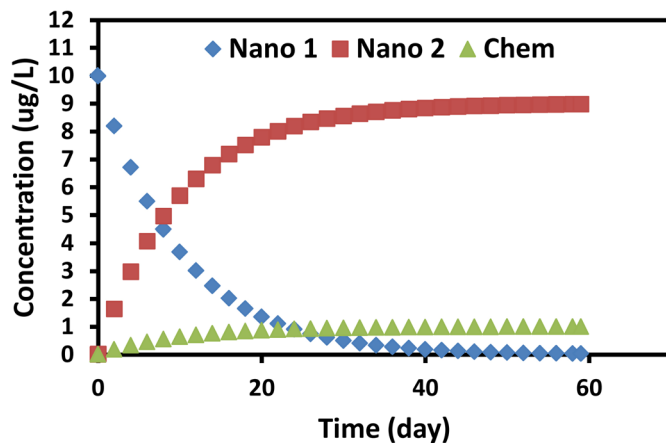


Figure 10. Nanomaterial parallel reaction simulation results using WASP8

the system. For a river divided into different segments along the mainstem, users can adjust reaction rates in different segments using the segment multiplication factor. Besides reaction rate, the segment multiplication factor can be used to adjust other model parameters in different segments (e.g., water temperature, solar radiation intensity, wind speed, etc.), and it is a convenient way to set the model parameters in WASP8.

For a river model divided into 8 segments along its mainstem, the temperature from segments 1 to 8 is 20, 22, 16, 21, 23, 20, 25°C, respectively, in water column. WASP8 users can set a temperature of 20°C once in “Environmental Parameter” for water column, then turn on segment multiplication factor and set segment multiplication factors 1, 1.1, 0.9, 0.8, 1.05, 1.15, 1 and 1.25 from segments 1 to 8. The same method can set other parameters in different segments.

6.5.5. Phase Multiplication Factor

Using AgNP dissolution as an example, we show how to use the phase multiplication factor to adjust the nanomaterial reaction rate constant. Studies indicate that nanomaterials coated with polymer or DOC can stabilize nanomaterial in the environment, which prevents them from aggregating and reducing the dissolution or oxidation rate. Nanomaterial surfaces coated with DOC in surface waters is common. This process may reduce the nanomaterial dissolution rate.

Assuming that surfaces of all AgNPs in surface waters are covered by DOC, and that this surface modification reduces the dissolution rate two-fold, compared to pristine AgNPs, the phase multiplication factor can be written as

$$X_{phase} = f_{doc} x_{doc} = 0.5 \quad \text{Equation 92}$$

so the dissolution rate is

$$k_{reaction} = k_{rate} X_{phase} = 0.5 k_{rate} \quad \text{Equation 93}$$

We still use data from WASP8 simulation results of the AgNP dissolution example. Dissolution rate is 0.0542 hour^{-1} for 40 nm-300 $\mu g/L$ AgNPs group, and 0.0487 hour^{-1} for 80 nm-600 $\mu g/L$ AgNPs group. Keeping the same dissolution rate settings in WASP, we set f_{doc} as 1 and x_{doc} as 0.5; simulation results are presented in Figure 11.

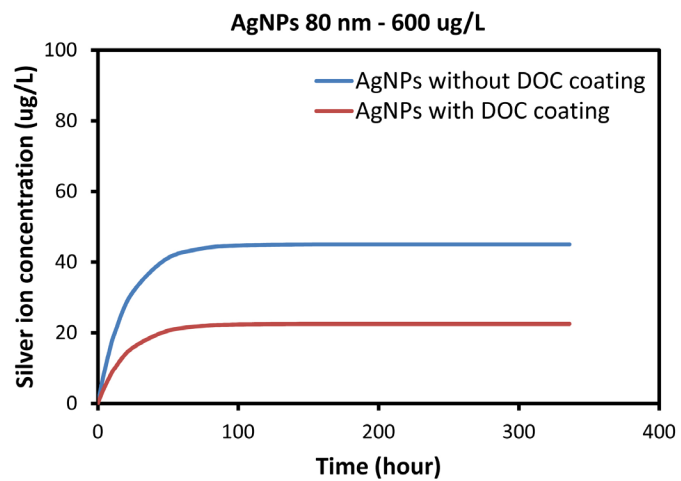
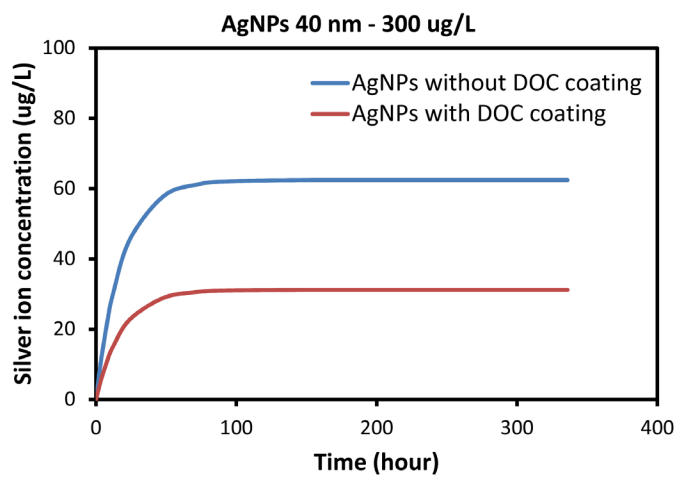


Figure 11. WASP8 simulation results.

7.0

Dissolved Chemicals Reactions

7.1. Introduction

Distribution and concentrations of dissolved contaminants in surface waters are significantly influenced by interactions between contaminants and the physical and chemical components of aquatic environments. These fate processes must be fully assessed during the evaluation of contaminant fate and transport to accurately simulate the behavior of contaminants in surface waters. Oxidation-reduction (redox) reactions, biodegradation and photochemical reactions account for a range of chemical reactions that occur in surface waters (e.g., rivers, lakes, sediments). Redox reactions involve oxidation and reduction, which occur with the exchange of electrons between reacting chemical species. Electrons are lost in oxidation, and gained in reduction. Organic contaminants of concern such as aromatic hydrocarbons, aldehydes, ketones, phenols, hydroquinones, and aliphatics are susceptible to oxidation. Typical reductive transformation of environmental contaminants includes dehalogenation of chlorinated aliphatic or aromatic contaminants and reduction of nitroaromatic compounds. Typical environmental oxidants include oxygen, ozone, chlorine dioxide, ferrate, and chromate; typical environmental reductants include low molecular weight organics, dithionite, sulfides (and polysulfides), Fe(II) at mineral surfaces, and zero-valent iron. Biodegradation refers to the conversion to mineralized end products (e.g., CO₂, H₂O and salts) through metabolism by living organisms, an important process for removing organic contaminants in surface waters and sediment. Phototransformation refers to a chemical reaction initiated by the absorption of energy in the form of light; most phototransformations occurring in surface water is driven by sunlight radiation.

WASP8 includes biodegradation, oxidation, and reduction and photochemical reactions. The previous WASP version (WASP7) can simulate these four chemical reactions for up to three chemical state variables, but WASP8 allows simulation of up to 10 variables and handles more complicated situations.

7.2. Simulation for Oxidation, Reduction and Biodegradation

7.2.1. Generic Reaction Module

Oxidation, reduction, and biodegradation reaction uses a generic transformation reaction and is constructed as:

$$k_{reaction} = k_{rate} X_{temp} X_{seg} X_{phase} X_{monod_conc} X_{monod_env}$$

Equation 94

where $k_{reaction}$ is the overall reaction rate constant (d⁻¹) that WASP8 calculates, k_{rate} is first-order reaction rate constant (d⁻¹) at 20°C, X_{temp} is the temperature correction factor, X_{seg} is the segment multiplication factor, X_{phase} is the phase multiplication factor, X_{monod_conc} is Monod equation and X_{monod_env} is Monod environmental reactant corrector. k_{rate} is first-order reaction rate constant at 20°C that needs to be input into WASP8. Default values are 1 for the other five terms in Equation 96 if reaction rate is not affected by them. If the reaction rate is influenced by other terms, WASP8 users must activate them and input the correct values.

7.2.2. Effect of Temperature

X_{temp} is the temperature correction factor when temperature affects the reaction rate, expressed as

$$X_{temp} = \theta^{(T-20)} \quad \text{Equation 95}$$

where θ is temperature-activity coefficient, and T is temperature (°C).

7.2.3. Phase Multiplication Factor

X_{phase} is used when the reaction only occurs for specific phases. For example, if a contaminant in aqueous environment is sorbed on a suspended solid, its reaction rate may be different than that in dissolved form. Phase multiplication factor is thus designed and expressed as

$$X_{phase} = f_{diss} x_{diss} + f_{doc} x_{doc} + f_{solid} x_{solid} \quad \text{Equation 96}$$

where f_{diss} , f_{doc} , and f_{solid} are the mass fractions of the contaminant in its dissolved form, DOC-complexed form, and the contaminant sorbed on solid phase, respectively; x_{diss} , x_{doc} , and x_{solid} are phase multiplication factors for the contaminant in its dissolved form, DOC-complexed form, and sorbed form.

Mass fractions of the contaminant in three different forms are determined by their partition coefficients, and their relation is

$$f_{diss} + f_{doc} + f_{solid} = 1 \quad \text{Equation 97}$$

Default values for three phase multiplication factors are 1 in WASP8.

7.2.4. Segment Multiplication Factor

Similarly to nanomaterial reaction, segment multiplication factor adjusts chemical reaction rates in different segments in the modeled region. Methods are described in a previous chapter.

7.2.5. Monod Kinetics

X_{conc} is the factor that accounts for Monod-type kinetics as a function of the nanomaterial structure. This is structured in WASP as follows:

$$X_{conc} = \frac{K_m}{K_m + C} \quad \text{Equation 98}$$

where K_m is the Monod half-saturation coefficient (mg/L). This is structured so that the base reaction rate constant, k_{rate} , must be adjusted so the maximum reaction rate is k_{rate}/K_m .

7.2.6. Environmental Kinetics

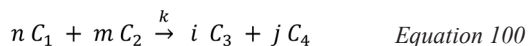
Similarly to Monod kinetics, environmental factors can be incorporated into the reaction rate using X_{env} . This can be used to incorporate oxidation with oxygen, for example and is structured in WASP as

$$X_{env} = \frac{E_x}{K_e + E_x} \quad \text{Equation 99}$$

where E_x is the environmental concentration of interest (mg/L) (e.g., oxygen, sulfate) and K_e is the half-saturation coefficient for this environmental parameter. The use of this functionality requires an E-option switch of 1, 2, or 3. If the switch is 1, then this is not used, and $X_{env} = 1$. If the switch is 2, then it is modeled as first order, and $X_{env} = E_x$. If the switch is 3, then $X_{env} = E_x/K_e + E_x$ Equation 80 is used.

7.2.7. Second Order Kinetics

For chemical reactions, second order kinetics can also be implemented. For this case, the stoichiometry of the reaction is important.



where n , m , i , and j are molar quantities input in the new constant group: Chemical Second Order Rxn. Chemical reactant and product identifiers are also input, along with reaction rate constant, temperature correction constants, and phase efficiencies. The reaction is of the form:

$$\frac{dC_1}{dt} = k C_2^{m/n} C_1 \quad \text{Equation 101}$$

The reaction yields [g/g] include the consumption of C_1 and production of C_3 and C_4 . These are calculated from the molar stoichiometry and molecular weights.

7.2.8. Biodegradation

When degradation of dissolved chemical is through biodegradation reaction, Monod kinetics can be used to simulate biodegradation, and X_{monod_conc} is expressed as follows:

$$X_{monod_conc} = \frac{K_s}{K_s + C} X \quad \text{Equation 102}$$

where X is the biomass concentration (mg/L), C is the limiting substrate concentration (mg/L), K_s is the half-saturation coefficient (mg/L). The way this is structured is such that the base reaction rate constant, k_{rate} , needs to be adjusted so that the maximum reaction rate is k_{rate}/K_s . This

allows the Monod relation to collapse to first order at low substrate concentrations. When this occurs, $C \ll K_s$, which is common in surface waters, the reaction becomes

$$k_{reaction} = k_{rate} \frac{K_s X}{K_s + C} \approx k_{rate} \frac{K_s}{K_s} X = k_{rate} X \quad \text{Equation 103}$$

where k_{rate} is the maximum substrate utilization rate (d^{-1}) in Monod equation, and k' is first-order kinetic reaction rate constant (d^{-1}).

In biodegradation module, WASP8 offers users two alternatives to model biodegradation: Users can either directly input first-order reaction rate constant, or input all the parameters in Monod equation into WASP8.

Dissolved oxygen, nitrate or other environmental reactants can influence enzyme metabolism activity and, thus, biodegradation. The effect of possible environmental reactants on the biokinetic is accounted for by one correction factor, expressed as X_{monod_env} , in the form of one saturation term:

$$X_{monod_env} = \frac{E}{K_{env} + E} \quad \text{Equation 104}$$

where E is the environmental reactant concentration (mg/L), and K_{env} is the half-saturation coefficient of environmental reactant (mg/L).

7.3. Dissolved Chemicals Phototransformation

The dissolved chemical phototransformation module is the same as the nanomaterial phototransformation module: reaction follows first-order kinetic reaction and the light spectrum is divided into 10 specific wavelengths. WASP8 calculates a phototransformation rate for each wavelength first, and then aggregates them.

Dissolved chemical phototransformation is expressed as follows:

$$\frac{dC}{dt} = -k_{photo} C \quad \text{Equation 105}$$

where k_{photo} is phototransformation rate (d^{-1}) that WASP8 calculates, and C is chemical concentration (mg/L). The overall photoreaction rate constant is expressed as

$$k_{photo} = \sum_{\lambda=1}^{10} (k_{photo,\lambda}) \quad \text{Equation 106}$$

where k_{photo} is the overall phototransformation rate constant (d^{-1}), and $k_{photo,\lambda}$ is phototransformation rate constant for specific wavelength (d^{-1}).

7.4. Examples

7.4.1. First-Order Biodegradation Influenced by Temperature

When temperature influences reaction rate, the temperature corrector must be turned on. WASP8's default setting is that when temperature is 20°C, reaction rate is not affected. In this example, we examine biodegradation rates at 10°C, 20°C, and 32°C. We assume the reaction rate is 0.2 d^{-1} at 20°C, which can be set in "Constant Group." Initial dissolved

chemical concentration is 10 mg/L. At a temperature of 20°C, the temperature corrector is not needed, but at temperatures of 10°C and 30°C, users must consider temperature's effect.

In general, when temperature influences on reaction rate, the reaction rate constant is expressed as

$$k_{reaction} = k_{rate}X_{temp} = k_{rate}\theta^{(T-20)} \quad \text{Equation 107}$$

For biodegradation, typical values for θ vary from 1.020 to 1.10. In WASP8, we set θ as 1.020 and temperature (T) can be set in "Constant Group."

The dissolved chemical biodegradation rate is

$$\frac{dC}{dt} = -k_{reaction}C \quad \text{Equation 108}$$

Its analytical solution is

$$C_t = C_{initial}(1 - \exp(k_{reaction}t)) \quad \text{Equation 109}$$

where C_t is dissolved chemical concentration (mg/L) at a given time, and $C_{initial}$ is initial dissolved chemical concentration (mg/L). Simulation results are shown in the following figure.

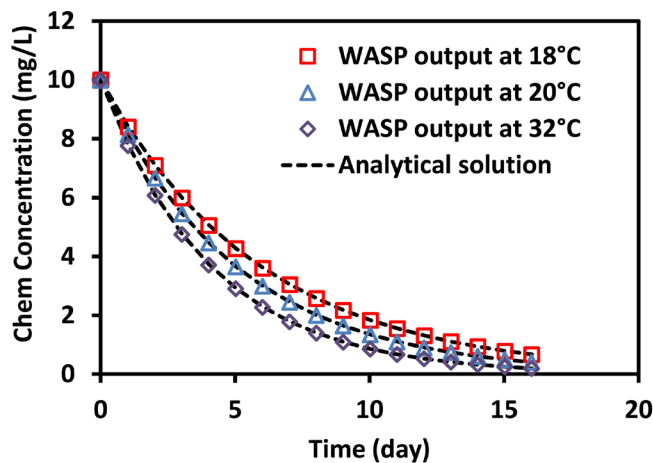


Figure 12. WASP8 output of biodegradation rate at different temperatures, fitted with analytical solution

7.4.2. Second-Order Reaction

WASP8 simulates second-order kinetic reaction by turning on the second-order kinetics option. Here, we use hydrogen peroxide (H_2O_2) decomposition reaction as an example. H_2O_2 can decompose into water and oxygen as follows:



Suppose initial H_2O_2 contraction is 20 mg/L, and reaction rate k is 0.02 L/(mmol·d⁻¹).

Consumption of H_2O_2 and formation of O_2 are expressed as

$$\frac{d[H_2O_2]}{dt} = -k[H_2O_2][H_2O_2] \quad \text{Equation 111}$$

$$\frac{d[O_2]}{dt} = \frac{1}{2}k[H_2O_2][H_2O_2] \quad \text{Equation 112}$$

If WASP8 users only want to simulate the consumption of H_2O_2 and formation of O_2 , they create two chemical state variables, and then input the initial concentrations, molecular weights of these two state variables and second-order reaction rates into WASP8. Next, turn on second-order functionality and provide concentration of the second reactant, H_2O_2 . In these two differential equations, H_2O_2 and O_2 are in the unit of mmol/L. In WASP8, the default unit of chemical state variable is "mg/L." WASP8 simulation results are shown in the following figure.

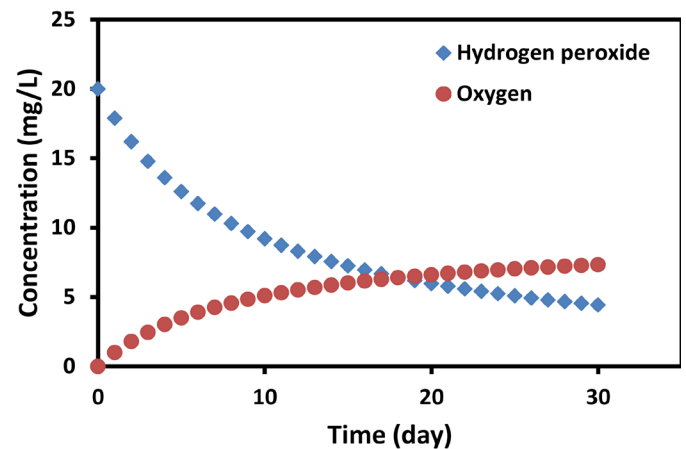


Figure 13. Second-order reaction simulation results by WASP8.

8.0

References

1. Knightes, C., Total maximum daily load (TMDL) for total mercury in fish tissue residue in the middle and lower Savannah River watershed U.S. Environmental Protection Agency. Region 4, A., GA., Ed. 2001.
2. Knightes, C., Total maximum daily load (TMDL) development for total mercury in fish tissue residue in the Canoochee River (Canoochee Watershed). U.S. Environmental Protection Agency. Region 4, A., GA., Ed. 2004.
3. Wang, P. F.; Martin, J.; Morrison, G., Water quality and eutrophication in Tampa Bay, Florida. *Estuarine, Coastal and Shelf Science* **1999**, *49* (1), 1-20.
4. U.S. EPA, Modeling Mercury Transport and Transformation along the Sudbury River, with Implications for Regulatory Action. Volume 2. Evaluating the Effectiveness of Different Remedial Alternatives to Reduce Mercury Concentrations in Fish. U.S. Environmental Protection Agency. Office of Research and Development. National Exposure Research Laboratory. Ecosystems Research Division. Athens, G., Ed. 2010 b.
5. U.S. EPA, Modeling Mercury Transport and Transformation along the Sudbury River, with. U.S. Environmental Protection Agency. Office of Research and Development. National Exposure Research Laboratory. Ecosystems Research Division. Athens, G., Ed. 2010 a.
6. Di Toro, D. M.; Fitzpatrick, J. J.; Thomann, R. V., Documentation for water quality analysis simulation program (WASP) and model verification program (MVP). **1983**.
7. Connolly, J. P.; Winfield, R. P., A user's guide for *WASTOX, a framework for modeling the fate of toxic chemicals in aquatic environments*. Environmental Research Laboratory, Office of Research and Development, US Environmental Protection Agency: 1984.
8. Ambrose, R. B.; Wool, T. A.; Connolly, J. P.; Schanz, R. W. *WASP4, a hydrodynamic and water-quality model-model theory, user's manual, and programmer's guide*; Environmental Protection Agency, Athens, GA (USA). Environmental Research Lab.: 1988.
9. Gee, G. W.; Bauder, J. W., Particle-size analysis. *Methods of soil analysis: Part I—Physical and mineralogical methods* **1986**, (methodsofsoilan1), 383-411.
10. Blake, G. R.; Hartge, K. H., Particle density. *Methods of Soil Analysis: Part I—Physical and Mineralogical Methods* **1986**, (methodsofsoilan1), 377-382.
11. Liu, B. Y. H.; Jordan, R. C., The interrelationship and characteristic distribution of direct, diffuse and total solar radiation. *Solar energy* **1960**, *4* (3), 1-19.
12. Duffie, J. A.; Beckman, W. A., Solar engineering of thermal processes. **1980**.
13. Iqbal, M., *An introduction to solar radiation*. Elsevier: 2012.
14. Swinehart, D. F., The beer-lambert law. *J. Chem. Educ* **1962**, *39* (7), 333.
15. Fuwa, K.; Valle, B. L., The Physical Basis of Analytical Atomic Absorption Spectrometry. The Pertinence of the Beer-Lambert Law. *Analytical Chemistry* **1963**, *35* (8), 942-946.
16. Bedient, P. B.; Rifai, H. S.; Newell, C. J., Ground water contamination: transport and remediation. **1994**.
17. Ho, Y.-S.; McKay, G., The kinetics of sorption of divalent metal ions onto sphagnum moss peat. *Water research* **2000**, *34* (3), 735-742.
18. Vadivelan, V.; Kumar, K. V., Equilibrium, kinetics, mechanism, and process design for the sorption of methylene blue onto rice husk. *Journal of colloid and interface science* **2005**, *286* (1), 90-100.
19. Karickhoff, S. W., Organic pollutant sorption in aquatic systems. *Journal of hydraulic engineering* **1984**, *110* (6), 707-735.
20. Arvidsson, R.; Molander, S.; Sandén, B. A.; Hassellöv, M., Challenges in exposure modeling of nanoparticles in aquatic environments. *Human and ecological risk assessment* **2011**, *17* (1), 245-262.

21. Praetorius, A.; Scheringer, M.; Hungerbühler, K., Development of Environmental Fate Models for Engineered Nanoparticles –A Case Study of TiO₂ Nanoparticles in the Rhine River. *Environmental science & technology* **2012**, *46* (12), 6705-6713.
22. Auffan, M.; Rose, J.; Bottero, J.-Y.; Lowry, G. V.; Jolivet, J.-P.; Wiesner, M. R., Towards a definition of inorganic nanoparticles from an environmental, health and safety perspective. *Nature nanotechnology* **2009**, *4* (10), 634-641.
23. Iso, N., Terminology and definitions for nano-objects–Nanoparticle, nanofibre and nanoplate. *ISO/TS 2008*, 27687.
24. Commission, E. U., Commission Recommendation of 18 October 2011 on the definition of nanomaterial (2011/696/EU). *Official Journal of the European Communities: Legis* **2011**.
25. Tratnyek, P. G.; Johnson, R. L., Nanotechnologies for environmental cleanup. *Nano Today* **2006**, *1* (2), 44-48.
26. Weir, A.; Westerhoff, P.; Fabricius, L.; Hristovski, K.; Von Goetz, N., Titanium dioxide nanoparticles in food and personal care products. *Environmental science & technology* **2012**, *46* (4), 2242-2250.
27. Li, X.-q.; Elliott, D. W.; Zhang, W.-x., Zero-valent iron nanoparticles for abatement of environmental pollutants: Materials and engineering aspects. *Critical Reviews in Solid State and Materials Sciences* **2006**, *31* (4), 111-122.
28. Rasmussen, J. W.; Martinez, E.; Louka, P.; Wingett, D. G., Zinc oxide nanoparticles for selective destruction of tumor cells and potential for drug delivery applications. *Expert opinion on drug delivery* **2010**, *7* (9), 1063-1077.
29. Lok, C.-N.; Ho, C.-M.; Chen, R.; He, Q.-Y.; Yu, W.-Y.; Sun, H.; Tam, P. K.-H.; Chiu, J.-F.; Che, C.-M., Silver nanoparticles: partial oxidation and antibacterial activities. *JBIC Journal of Biological Inorganic Chemistry* **2007**, *12* (4), 527-534.
30. Segal, M., Selling graphene by the ton. *Nature nanotechnology* **2009**, *4* (10), 612-614.
31. Zhang, D.; Ryu, K.; Liu, X.; Polikarpov, E.; Ly, J.; Tompson, M. E.; Zhou, C., Transparent, conductive, and flexible carbon nanotube films and their application in organic light-emitting diodes. *Nano letters* **2006**, *6* (9), 1880-1886.
32. Chowdhury, I.; Hou, W.-C.; Goodwin, D.; Henderson, M.; Zepp, R. G.; Bouchard, D., Sunlight affects aggregation and deposition of graphene oxide in the aquatic environment. *Water research* **2015**, *78*, 37-46.
33. Hou, W.-C.; Chowdhury, I.; Goodwin Jr, D. G.; Henderson, W. M.; Fairbrother, D. H.; Bouchard, D.; Zepp, R. G., Photochemical transformation of graphene oxide in sunlight. *Environmental science & technology* **2015**, *49* (6), 3435-3443.
34. Whitley, A. R.; Levard, C.; Oostveen, E.; Bertsch, P. M.; Matocha, C. J.; Kammer, F. v. d.; Unrine, J. M., Behavior of Ag nanoparticles in soil: Effects of particle surface coating, aging and sewage sludge amendment. *Environmental Pollution* **2013**, *182*, 141-149.
35. Miao, A. J.; Zhang, X. Y.; Luo, Z.; Chen, C. S.; Chin, W. C.; Santschi, P. H.; Quigg, A., Zinc oxide–engineered nanoparticles: Dissolution and toxicity to marine phytoplankton. *Environmental Toxicology and Chemistry* **2010**, *29* (12), 2814-2822.
36. Xia, T.; Kovoichich, M.; Liong, M.; Mädler, L.; Gilbert, B.; Shi, H.; Yeh, J. I.; Zink, J. I.; Nel, A. E., Comparison of the mechanism of toxicity of zinc oxide and cerium oxide nanoparticles based on dissolution and oxidative stress properties. *ACS nano* **2008**, *2* (10), 2121-2134.
37. Leupin, O. X.; Hug, S. J., Oxidation and removal of arsenic (III) from aerated groundwater by filtration through sand and zero-valent iron. *Water Research* **2005**, *39* (9), 1729-1740.
38. Xie, Y.; Cwiertny, D. M., Use of Dithionite to Extend the Reactive Lifetime of Nanoscale Zero-Valent Iron Treatment Systems. *Environmental Science & Technology* **2010**, *44* (22), 8649-8655.
39. Dale, A. L.; Lowry, G. V.; Casman, E. A., Stream dynamics and chemical transformations control the environmental fate of silver and zinc oxide nanoparticles in a watershed-scale model. *Environmental science & technology* **2015**, *49* (12), 7285-7293.
40. Levard, C.; Hotze, E. M.; Colman, B. P.; Dale, A. L.; Truong, L.; Yang, X. Y.; Bone, A. J.; Brown Jr, G. E.; Tanguay, R. L.; Di Giulio, R. T., Sulfidation of silver nanoparticles: natural antidote to their toxicity. *Environmental science & technology* **2013**, *47* (23), 13440-13448.
41. Levard, C.; Reinsch, B. C.; Michel, F. M.; Oumahi, C.; Lowry, G. V.; Brown Jr, G. E., Sulfidation processes of PVP-coated silver nanoparticles in aqueous solution: impact on dissolution rate. *Environmental science & technology* **2011**, *45* (12), 5260-5266.
42. Metcalf; Eddy, *Wastewater engineering: treatment and reuse*. McGraw-Hill: 2003.
43. Glazer, A. N., Light guides. Directional energy transfer in a photosynthetic antenna. *Journal of Biological Chemistry* **1989**, *264* (1), 1-4.
44. Hasnat, M. A.; Uddin, M. M.; Samed, A. J. F.; Alam, S. S.; Hossain, S., Adsorption and photocatalytic decolorization of a synthetic dye erythrosine on anatase TiO₂ and ZnO surfaces. *Journal of Hazardous Materials* **2007**, *147* (1–2), 471-477.

45. Sahoo, C.; Gupta, A. K.; Pal, A., Photocatalytic degradation of Methyl Red dye in aqueous solutions under UV irradiation using Ag⁺ doped TiO₂. *Desalination* **2005**, *181* (1–3), 91-100.
46. Houas, A.; Lachheb, H.; Ksibi, M.; Elaloui, E.; Guillard, C.; Herrmann, J.-M., Photocatalytic degradation pathway of methylene blue in water. *Applied Catalysis B: Environmental* **2001**, *31* (2), 145-157.
47. Canonica, S.; Meunier, L.; Von Gunten, U., Phototransformation of selected pharmaceuticals during UV treatment of drinking water. *Water Research* **2008**, *42* (1), 121-128.
48. Stephens, G. L.; Li, J.; Wild, M.; Clayson, C. A.; Loeb, N.; Kato, S.; L'Ecuyer, T.; Stackhouse Jr, P. W.; Lebsack, M.; Andrews, T., An update on Earth's energy balance in light of the latest global observations. *Nature Geoscience* **2012**, *5* (10), 691-696.
49. Yang, X.; Gondikas, A. P.; Marinakos, S. M.; Auffan, M.; Liu, J.; Hsu-Kim, H.; Meyer, J. N., Mechanism of silver nanoparticle toxicity is dependent on dissolved silver and surface coating in *Caenorhabditis elegans*. *Environmental science & technology* **2011**, *46* (2), 1119-1127.
50. Kittler, S.; Greulich, C.; Diendorf, J.; Köller, M.; Epple, M., Toxicity of silver nanoparticles increases during storage because of slow dissolution under release of silver ions. *Chem. Mater* **2010**, *22* (16), 4548-4554.
51. Liu, J.; Hurt, R. H., Ion release kinetics and particle persistence in aqueous nano-silver colloids. *Environ. Sci. Technol* **2010**, *44* (6), 2169-2175.
52. Hassellöv, M.; Readman, J. W.; Ranville, J. F.; Tiede, K., Nanoparticle analysis and characterization methodologies in environmental risk assessment of engineered nanoparticles. *Ecotoxicology* **2008**, *17* (5), 344-361.
53. Zhang, W.; Yao, Y.; Sullivan, N.; Chen, Y., Modeling the primary size effects of citrate-coated silver nanoparticles on their ion release kinetics. *Environmental science & technology* **2011**, *45* (10), 4422-4428.
54. Peretyazhko, T. S.; Zhang, Q.; Colvin, V. L., Size-controlled dissolution of silver nanoparticles at neutral and acidic pH conditions: kinetics and size changes. *Environmental science & technology* **2014**, *48* (20), 11954-11961.
55. Zhang, W.; Yao, Y.; Li, K.; Huang, Y.; Chen, Y., Influence of dissolved oxygen on aggregation kinetics of citrate-coated silver nanoparticles. *Environmental Pollution* **2011**, *159* (12), 3757-3762.
56. Martin, M. N.; Allen, A. J.; MacCuspie, R. I.; Hackley, V. A., Dissolution, agglomerate morphology, and stability limits of protein-coated silver nanoparticles. *Langmuir* **2014**, *30* (38), 11442-11452.
57. Dale, A. L.; Lowry, G. V.; Casman, E. A., Modeling nanosilver transformations in freshwater sediments. *Environ. Sci. Technol* **2013**, *47* (22), 12920-12928.

9.0 APPENDIX

9.1 Solids QA/QC

Table 11. Parameters used in Analytical Equations

Variable	Description	Units
Q_{in}	Flow in	m ³ /d
Q_{out}	Flow out	m ³ /d
V^{WC}	Water Column Volume	m ³
V^S	Sediment Layer Volume	m ³
v_s	Settling Velocity	m/d
v_r	Resuspension Velocity	m/d
A_{bed}	Cross-sectional Area of Bed	m ²
S_j^{WC}	Concentration of Solid j in Water Column	mg/L
S_j^s	Concentration of Solid j in Sediments	mg/L
$S_{o,j}^{WC}$	Initial Concentration of Solid j	mg/L
$S_{BC,j}^{WC}$	Boundary Condition Concentration of Solid j	mg/L
t	Time	d

A two-segment WASP model (consisting of a water column and sediment layer below) simulated solids processes for comparing analytical solutions to WASP simulation results. Table 12 shows the channel geometry of the segments.

Table 12. Channel Geometry of WASP Segment

Segment	Water Column	Sediments
Volume	100,000 m ³	500 m ³
Length	100 m	100 m
Depth	10 m	0.05 m
Width	100 m	100 m

To ensure quality assurance of the solids module, we tested boundary condition (BC) and initial condition (IC) of solids concentrations, Stokes' settling, and resuspension. For both BC and IC scenarios, we simulated a single solid with streamflow moving through the segment. Settling was simulated with 10 solids simultaneously, varying streamflow and settling velocities. Resuspension was simulated using a single solid with no flow.

9.1.1. Scenario 1 – Constant Boundary Conditions, Initial Concentration = 0, No Settling

Using a solid boundary condition of 10 mg/L, we modeled the increase of concentration over time. With no initial solid concentration, and a steady state streamflow, the analytical equation for this problem is defined as:

$$V^{WC} \frac{\Delta S_j^{WC}}{\Delta t} = Q_{in} S_{BC,j}^{WC} - Q_{out} S_{out,j}^{WC} \quad \text{Equation 113}$$

where:

$$S_{0,j}^{WC} = 0 \text{ mg/L}$$

$$S_{BC,j}^{WC} = 10 \text{ mg/L}$$

$$Q_{in} = Q_{out} = 172,800 \text{ m}^3/\text{d}$$

$$V^{WC} = 100,000 \text{ m}^3$$

At steady state, $Q=Q_{in}=Q_{out}$. We solve for $S_{out,j}^{WC}$, where the concentration flowing out equals the concentration in the water column ($S_j^{WC}=S_{out,j}^{WC}$), to get:

$$S_{out,i}^{WC} = S_{BC,i}^{WC} - S_{BC,i}^{WC} e^{(-\frac{Q_{in} t}{V^{WC}})} \quad \text{Equation 114}$$

Figure 14 shows the comparison of WASP simulation to analytical solution. WASP outputs were set to a 0.1/d time step, about two and a half hours.

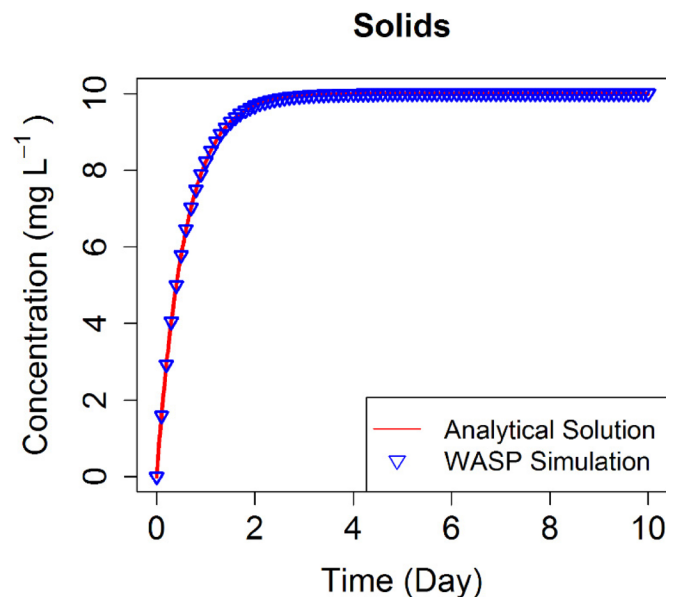


Figure 14. Comparison of WASP Simulation to Analytical Solution for Scenario 1

9.1.2. Scenario 2 - Initial Conditions, Boundary Condition = 0, No Settling

Similarly to the BC scenario, an initial solid concentration modeled the decrease of concentrations over time. With no BC input and a steady state flow, the analytical equation for this problem is defined as:

$$V^{WC} \frac{\Delta S_j^{WC}}{\Delta t} = -Q_{out} S_{out,j}^{WC} \quad \text{Equation 115}$$

where:

$$S_{0,j}^{WC} = 10 \text{ mg/L}$$

$$S_{BC,j}^{WC} = 0 \text{ mg/L}$$

$$Q_{in} = Q_{out} = 172,800 \text{ m}^3/\text{d}$$

$$V^{WC} = 100,000 \text{ m}^3$$

Solving for S_i^{WC} we get:

$$S_j^{WC} = S_{0,j}^{WC} e^{(-\frac{Q_{out}}{V^{WC}})t} \quad \text{Equation 116}$$

Figure 15 shows the comparison of WASP simulation to analytical solution.

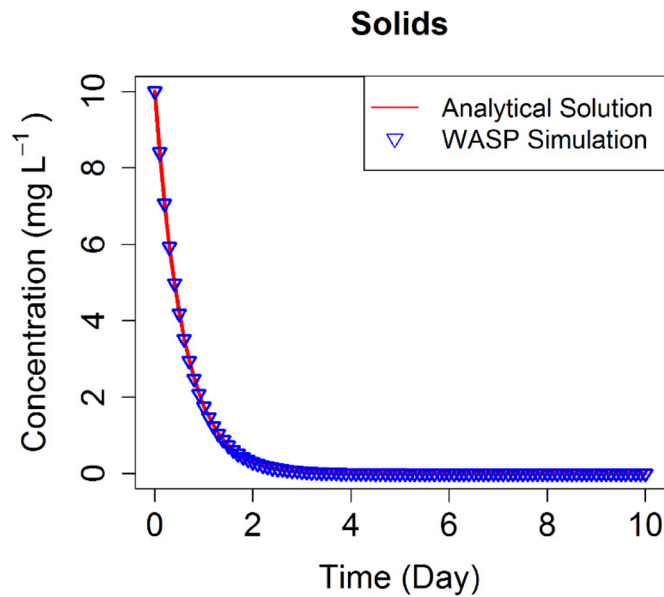


Figure 15. Comparison of WASP Simulations to Analytical Solutions for Scenario 2

9.1.3. Scenario 3 – Initial Concentration, With and Without Streamflow, Settling

We tested settling scenarios with and without streamflow. Because settling can be simulated with multiple solids independently, we were able to simulate 10 solids simultaneously settling. For the first scenario, we simulated 10 solids, all with different settling velocities and all with an initial concentration of 10 mg/L, and no streamflow. Descriptive settling rates were applied to each solid using:

$$v_{set}^{particle} = \frac{2}{9} g \frac{(\rho_{particle} - \rho_{water})}{\mu_{water}} r_{particle}^2 \quad \text{Equation 117}$$

Table 13 lists properties for the 10 solids used in scenario 3.

Table 13. Physical properties of solids

Solid	Density (mg/L)	Particle Radius (mm)	Settling Velocity (m/d)
1	2.65	8.97E-04	0.25
2	2.65	1.27E-03	0.5
3	2.65	1.79E-03	1
4	2.65	4.01E-03	5
5	2.65	8.97E-03	25
6	2.65	1.27E-02	50
7	2.65	1.79E-02	100
8	2.65	2.20E-02	150
9	2.65	2.54E-02	200
10	2.65	2.84E-02	250

Settling can be described with the mass balance equation:

$$V^{WC} \frac{\Delta S_j^{WC}}{\Delta t} = -Q_{out} S_{out,j}^{WC} - v_s A_{bed} S_j^{WC} \quad \text{Equation 118}$$

where:

$$S_{0,j}^{WC} = 10 \text{ mg/L for solids 1-10}$$

$$v_s = 0.25, 0.5, 1, 5, 25, 50, 100, 150, 200, 250 \text{ m/d}$$

$$A_{bed} = 10000 \text{ m}^2$$

$$Q_{in} = Q_{out} = 0; 172,800 \text{ m}^3/\text{d}$$

$$V^{WC} = 100,000 \text{ m}^3$$

Solving for S_j^{WC} to get:

$$S_j^{WC} = S_{0,j}^{WC} e^{-(\frac{Q_{out} + v_s A_{bed}}{V^{WC}})t} \quad \text{Equation 119}$$

Figure 16 shows the output comparison of all 10 solids modeled in WASP when $Q_{in} = Q_{out} = 172,800 \text{ m}^3/\text{d}$.

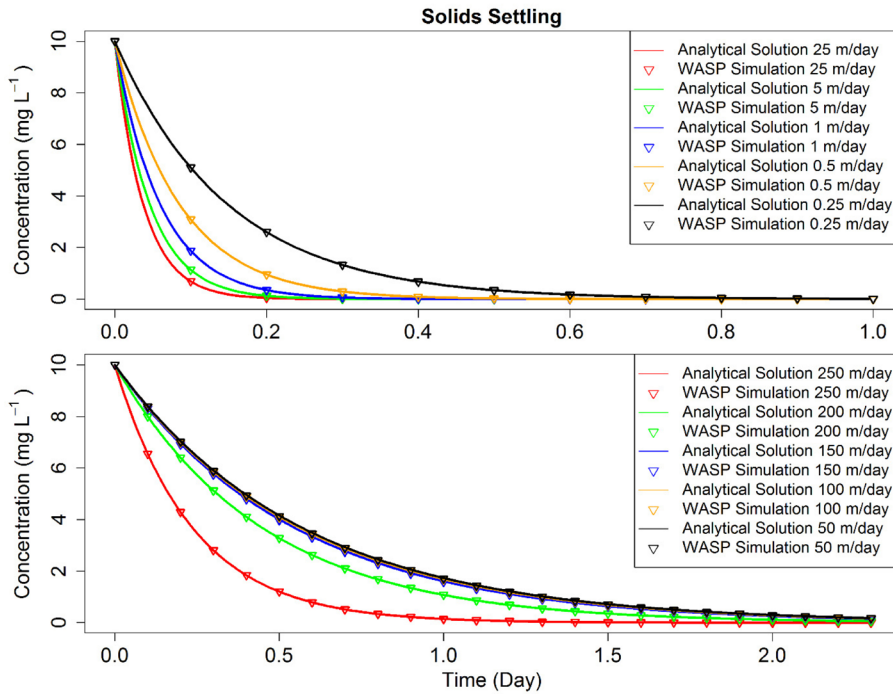


Figure 16. Comparison of WASP Simulations to Analytical Solutions for Scenario 3, With Streamflow

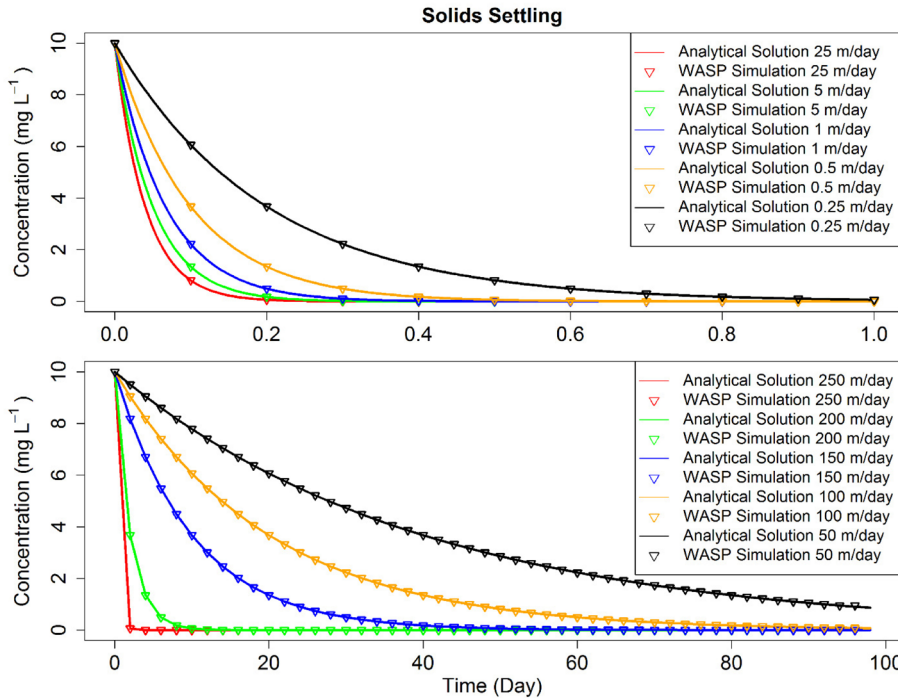


Figure 17. Comparison of WASP Simulations to Analytical Solutions for Scenario 3, Without Streamflow

In the scenario where $Q = 0$ the solution can be simplified:

$$S_j^{WC} = S_{0,j}^{WC} e^{\left(\frac{-v_s A_{bed} t}{V^{WC}}\right)} \quad \text{Equation 120}$$

Figure 17 shows the output comparison of all 10 solids modeled in WASP when $Q = 0 \text{ m}^3/\text{d}$.

9.1.4. Scenario 4 - Resuspension

Simulating resuspension analytically is more complicated because all solids concentrations in sediments affect the concentration of an individual solid that is being resuspended. We therefore modeled a single solid being resuspended from the sediment layer into the water column. This demonstrates the processes in WASP8 and tests if code is working properly.

Resuspension from the sediment layer can be described with the mass balance equation:

$$V^S \frac{\Delta S_j^S}{\Delta t} = -v_r A_{bed} S_j^S \quad \text{Equation 121}$$

where:

$$Q = 0$$

$$V^S = 500 \text{ m}^3$$

We simplify and differentiate to solve:

$$S_j^S = S_{0,j}^S e^{\frac{v_r A_{bed} S_j^S t}{V^S}} \quad \text{Equation 122}$$

Figure 18. Shows the solid concentration in sediments over time.

Solids in the Sediments

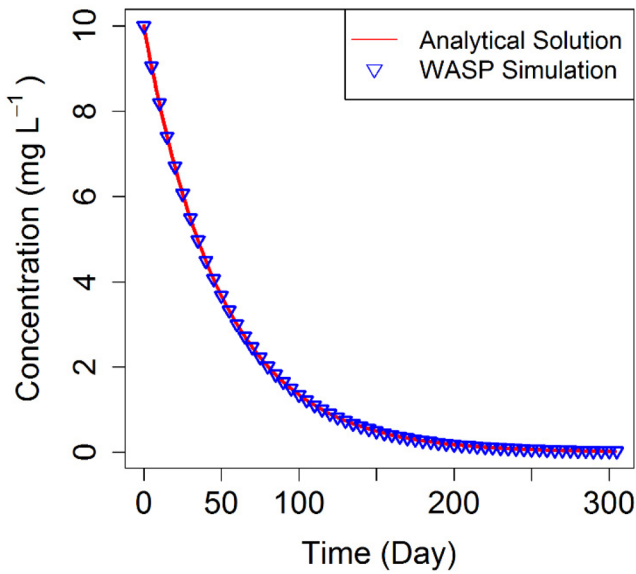


Figure 18. Comparison of WASP Simulations to Analytical Solutions for Scenario 4, Solids in Sediment Layer

Concentration in the water column can be described by the differential equation:

$$V^S \frac{dS_j^S}{dt} = -v_r A_{bed} S_j^S \quad \text{Equation 123}$$

where S_j^{WC} at time t is equal to:

$$S_{t,j}^{WC} = \frac{(S_{0,j}^S - S_{t,j}^S) V^S}{V^{WC}} \quad \text{Equation 124}$$

Figure 19 shows the solid concentration in the water column over time.

9.2. Light QA/QC

A WASP model consisting of two stacked water column segments simulated light processes for comparing analytical solutions to WASP simulation results. Table 14 shows the channel geometry of the segments.

Table 14. Channel Geometry of WASP Segments

Segment	Surface Water Column	Subsurface Water Column
Volume [m ³]	10,000	10,000
Length [m]	100	100
Depth [m]	1	1
Width [m]	100	100

For each light option we tested parameters related to light attenuation above and below the water column. Water surface reflectance, canopy shading, and light extinction were considered in all three light options. Cloud cover was tested in option 0 and fraction of daily light was tested in option 2.

Solids in the Water Column

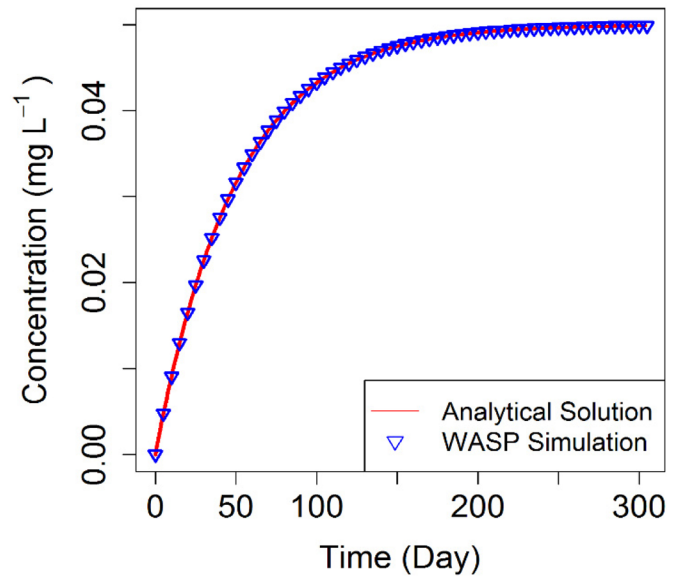


Figure 19. Comparison of WASP Simulations to Analytical Solutions for Scenario 4, Solids in Water Column

Table 15 lists the attenuation fraction for light groups and each light attenuation parameter value used for all three options, where applicable. Options 1 and 2 used a constant solar radiation time series of 100 W/m². For the chlorophyll scenario, algal chlorophyll was input as a constant 2 µg/L. An initial concentration in the surface water segment of 5 mg/L was used for the solids attenuation scenario and 4 mg/L for the DOC global attenuation scenario. For the DOC(i) scenario, a 3 mg/L initial concentration was used for DOC(1) in the surface water segment and a 2 mg/L initial concentration for DOC(2) in the subsurface water segment.

Table 15. Attenuation Fractions Used for Above Surface Parameters

Parameter	Input Value
Ultraviolet Light	0.036
PAR Light	0.464
Infrared Light	0.5
Surface Reflectance	0.15
Canopy Shading	0.2
Cloud Cover	0.4
Ice Cover	0.733
Light Extinction	0.5
Chlorophyll Extinction	0.8
Chlorophyll Exponent	0.1
Solids Extinction	0.5
DOC Global Extinction	0.6
DOC(1) Extinction	1
DOC(2) Extinction	2
Fraction of Day	0.5

Attenuation parameters below the water surface were tested with the average K_e for each light group, an output calculated internally by WASP, and applied to the Beer-Lambert equation (Equation 21). The average K_e outputs for each attenuation parameter, by light group, is listed in Table 16.

9.2.1. Option 0, Calculated Diel Light

Using coordinates from Athens, GA (33.9519, -83.3576), the model is simulated for a single day to get outputs for UV, PAR, and IR at the top and bottom of each segment. Using default settings with no attenuators turned on, the output light for a single day in each segment is described by wavelength group in Table 17.

Table 16. Average K_e Outputs for Each Attenuation Parameter by Light Group

Segment	Parameter	K_{eUV}	K_{ePAR}	K_{eIR}
1	Light Extinction	0.051	0.5	2.07
	Chlorophyll	0.168	0.289	2.07
	Solids	2.551	2.789	4.57
	DOC Global	10.962	2.689	2.07
	DOC (i)	8.394	1.189	2.07
	Frac of Day	0.051	0.289	2.07
2	Light Extinction	0.051	0.5	2.07
	Chlorophyll	0.167	0.164	2.07
	Solids	0.051	0.164	2.07
	DOC Global	0.034	0.164	2.07
	DOC (i)	5.154	0.764	2.07
	Frac of Day	0.051	0.164	2.07

Table 17. WASP Outputs by Wavelength Group for Option 0 Using Athens, GA Coordinates

Segment	Time	UV	PAR	IR
Top of Surface	9:00	9.62	124.02	133.68
	12:00	15.63	201.42	217.05
	15:00	5.71	73.57	79.28
Bottom of Surface	9:00	8.89	93.79	16.86
	12:00	14.44	152.22	27.39
	15:00	5.27	55.60	10.00
Top of Subsurface	9:00	8.89	93.72	16.86
	12:00	14.44	152.22	27.39
	15:00	5.27	55.60	10.00
Bottom of Subsurface	9:00	8.22	79.93	2.13
	12:00	13.4	129.83	3.46
	15:00	4.88	47.42	1.26

Table 18 shows the comparison of WASP simulations and analytical solutions for light attenuation parameters, above and at the water surface in percent error. Table 19 and Table 20 show the comparison between WASP simulations and analytical solutions for light attenuation parameters, below the water surface in percent error.

Table 18. Comparison of WASP Outputs to Analytical Solutions for Above Surface Light Attenuation – Option 0

Segment	Time	Water Surface Reflection			Canopy Shading			Cloud Cover			Ice Cover		
		UV	PAR	IR	UV	PAR	IR	UV	PAR	IR	UV	PAR	IR
Top of Surface	9:00	0.00	0.00	0.00	-0.01	0.00	0.00	0.00	0.00	0.00	0.00	0.00	0.00
	12:00	0.00	0.00	0.00	0.00	0.00	0.00	0.00	0.00	0.00	0.00	0.00	0.00
	15:00	0.01	0.00	0.00	0.01	0.00	0.00	0.01	0.00	0.00	0.01	0.00	0.00
Bottom of Surface	9:00	0.00	0.00	0.00	-0.01	0.00	0.00	0.00	0.00	0.00	0.00	0.00	0.00
	12:00	-0.01	0.00	0.00	-0.01	0.00	0.00	-0.01	0.00	0.00	-0.01	0.00	0.00
	15:00	0.00	0.00	0.00	-0.01	0.00	0.00	-0.01	0.00	0.00	-0.01	0.00	0.00
Top of Subsurface	9:00	0.00	0.00	0.00	0.00	0.00	0.00	0.00	0.00	0.00	0.00	0.00	0.00
	12:00	0.00	0.00	0.00	0.00	0.00	0.00	0.00	0.00	0.00	0.00	0.00	0.00
	15:00	0.00	0.00	0.00	0.00	0.00	0.00	0.00	0.00	0.00	0.00	0.00	0.00
Bottom of Subsurface	9:00	0.00	0.00	-0.01	-0.01	0.00	-0.02	0.00	0.00	0.02	0.01	0.00	-0.01
	12:00	0.00	0.00	0.00	0.00	0.00	0.01	0.00	0.00	0.01	-0.01	0.00	0.01
	15:00	0.00	0.00	0.07	0.02	0.00	0.04	0.01	0.00	0.02	0.02	0.00	0.00

Table 19. Comparison of WASP Outputs to Analytical Solutions for Below Surface Light Attenuation – Option 0

Segment	Date	Light Extinction			Chlorophyll		
		UV	PAR	IR	UV	PAR	IR
Bottom of Surface	9:00	-0.05	0.00	0.00	-0.04	-0.02	0.00
	12:00	-0.05	0.00	0.00	-0.03	-0.02	0.00
	15:00	-0.04	0.00	0.00	-0.03	-0.02	0.00
Top of Subsurface	9:00	0.00	0.00	0.00	0.00	0.00	0.00
	12:00	0.00	0.00	0.00	0.00	0.00	0.00
	15:00	0.00	0.00	0.00	0.00	0.00	0.00
Bottom of Subsurface	9:00	-0.01	0.00	0.01	0.01	0.02	0.01
	12:00	-0.01	0.00	0.00	-0.01	0.02	0.00
	15:00	-0.01	0.00	-0.03	0.00	0.02	-0.03

Table 20. Comparison of WASP Outputs to Analytical Solutions for Below Surface Light Attenuation – Option 0

Segment	Date	Solids			DOC Global			DOC (i)		
		UV	PAR	IR	UV	PAR	IR	UV	PAR	IR
Bottom of Surface	9:00	-0.07	-0.02	-0.01	0.04	-0.02	0.00	0.01	-0.02	0.00
	12:00	-0.09	-0.02	-0.01	0.03	-0.02	0.00	0.02	-0.02	0.00
	15:00	-0.05	-0.01	-0.02	0.02	-0.03	0.00	0.06	-0.02	0.00
Top of Subsurface	9:00	0.00	0.00	0.00	0.00	0.00	0.00	0.00	0.00	0.00
	12:00	0.00	0.00	0.00	0.00	0.00	0.00	0.00	0.00	0.00
	15:00	0.00	0.00	0.00	0.00	0.00	0.00	0.00	0.00	0.00
Bottom of Subsurface	9:00	0.04	0.02	0.21	-0.07	0.02	0.01	0.04	0.02	0.01
	12:00	0.05	0.02	0.12	-0.05	0.02	0.00	0.03	0.02	0.00
	15:00	0.03	0.00	0.39	-0.03	0.02	-0.03	-0.03	0.02	-0.03

Table 21. Comparison of WASP Outputs to Analytical Solutions for Above Surface Light Attenuation – Option 1

Segment	Water Surface Reflection			Canopy Shading			Ice		
	UV	PAR	IR	UV	PAR	IR	UV	PAR	IR
Top of Surface	0.00	0.00	0.00	-0.01	0.00	0.00	0.02	0.00	0.00
Bottom of Surface	-0.06	-0.02	0.00	-0.05	-0.02	0.01	-0.07	-0.01	0.00
Top of Subsurface	0.00	0.00	0.00	0.00	0.00	0.00	0.00	0.00	0.00
Bottom of Subsurface	0.02	0.02	0.04	-0.01	0.02	0.04	-0.02	0.01	0.09

9.2.2. Option 1, User Input Diel Light

Table 21 shows the comparison of WASP simulations and analytical solutions for light attenuation parameters, above and at the water surface in percent error.

Table 22 and Table 23 show the comparison of WASP simulations and analytical solutions for light attenuation parameters, below the water surface in percent error.

9.2.3. Option 2, User Input Daily Light, Calculated Diel Light

Using coordinates from Athens, GA (33.9519, -83.3576), the model is simulated for a single day to get outputs for UV, PAR, and IR at the top and bottom of each segment. Using default settings with no attenuators turned on, the output light for a single day in each segment is described by wavelength group in Table 24.

Table 22. Comparison of WASP Outputs to Analytical Solutions for Below Surface Light Attenuation – Option 1

Segment	Light Extinction			Chlorophyll		
	UV	PAR	IR	UV	PAR	IR
Top of Surface	0.00	0.00	0.00	0.00	0.00	0.00
Bottom of Surface	0.00	0.00	0.00	0.00	0.00	0.00
Top of Subsurface	0.00	0.00	0.00	0.00	0.00	0.00
Bottom of Subsurface	0.00	0.00	0.00	0.00	0.00	0.01

Table 23. Comparison of WASP Outputs to Analytical Solutions for Below Surface Light Attenuation – Option 1

Segment	Solids			DOC Global			DOC (i)		
	UV	PAR	IR	UV	PAR	IR	UV	PAR	IR
Top of Surface	0.00	0.00	0.00	0.00	0.00	0.00	0.00	0.00	0.00
Bottom of Surface	0.00	0.00	0.00	0.00	0.00	0.00	0.00	0.00	0.00
Top of Subsurface	0.00	0.00	0.00	0.00	0.00	0.00	0.00	0.00	0.00
Bottom of Subsurface	0.00	0.00	0.01	-0.01	0.00	0.01	-0.01	0.00	0.01

Table 24. WASP Outputs by Wavelength Group for Option 2 Using Athens, GA Coordinates

Segment	Time	UV	PAR	IR
Top of Surface	9:00	8.58	110.62	119.20
	12:00	13.94	179.66	193.60
	15:00	5.09	65.62	70.72
Bottom of Surface	9:00	7.93	83.59	15.04
	12:00	12.88	135.77	24.43
	15:00	4.70	49.59	8.92
Top of Subsurface	9:00	7.93	83.59	15.04
	12:00	12.88	135.77	24.43
	15:00	4.70	49.59	8.92
Bottom of Subsurface	9:00	7.34	71.30	1.90
	12:00	11.91	115.80	3.08
	15:00	4.35	42.30	1.13

Table 25 shows the comparison of WASP simulations and analytical solutions for light attenuation parameters above and at the water surface in percent error.

Table 26 and Table 27 show the comparison of WASP simulations and analytical solutions for light attenuation parameters, below the water surface in percent error.

Table 25. Comparison of WASP Outputs to Analytical Solutions for Above Surface Light Attenuation – Option 2

Segment	Time	Water Surface Reflection			Canopy Shading			Ice Cover		
		UV	PAR	IR	UV	PAR	IR	UV	PAR	IR
Top of Surface	9:00	0.00	0.00	0.00	-0.01	0.00	0.00	0.00	0.00	0.00
	12:00	0.00	0.00	0.00	0.00	0.00	0.00	0.00	0.00	0.00
	15:00	0.01	0.00	0.00	0.01	0.00	0.00	0.01	0.00	0.00
Bottom of Surface	9:00	0.00	0.00	0.00	-0.01	0.00	0.00	0.00	0.00	0.00
	12:00	-0.01	0.00	0.00	-0.01	0.00	0.00	-0.01	0.00	0.00
	15:00	0.00	0.00	0.00	-0.01	0.00	0.00	-0.01	0.00	0.00
Top of Subsurface	9:00	0.00	0.00	0.00	0.00	0.00	0.00	0.00	0.00	0.00
	12:00	0.00	0.00	0.00	0.00	0.00	0.00	0.00	0.00	0.00
	15:00	0.00	0.00	0.00	0.00	0.00	0.00	0.00	0.00	0.00
Bottom of Subsurface	9:00	0.00	0.00	-0.01	-0.01	0.00	-0.02	0.01	0.00	-0.01
	12:00	0.00	0.00	0.00	0.00	0.00	0.01	-0.01	0.00	0.01
	15:00	0.00	0.00	0.07	0.02	0.00	0.04	0.02	0.00	0.00

Table 26. Comparison of WASP Outputs to Analytical Solutions for Below Surface Light Attenuation – Option 2

Segment	Date	Light Extinction			Chlorophyll			Fraction of Day		
		UV	PAR	IR	UV	PAR	IR	UV	PAR	IR
Bottom of Surface	9:00	-0.05	0.00	0.00	-0.02	-0.02	0.00	-0.05	-0.02	0.00
	12:00	-0.04	0.00	0.00	-0.03	-0.02	0.00	-0.04	-0.02	0.00
	15:00	-0.05	0.00	0.00	-0.03	-0.02	0.00	-0.05	-0.02	0.00
Top of Subsurface	9:00	0.00	0.00	0.00	0.00	0.00	0.00	0.00	0.00	0.00
	12:00	0.00	0.00	0.00	0.00	0.00	0.00	0.00	0.00	0.00
	15:00	0.00	0.00	0.00	0.00	0.00	0.00	0.00	0.00	0.00
Bottom of Subsurface	9:00	0.00	0.00	-0.03	0.00	0.02	-0.03	0.00	0.02	-0.03
	12:00	-0.01	0.00	0.00	0.00	0.02	0.00	-0.01	0.02	0.00
	15:00	0.00	0.00	-0.03	-0.01	0.02	-0.03	0.00	0.02	-0.03

Table 27. Comparison of WASP Outputs to Analytical Solutions for Below Surface Light Attenuation – Option 2

Segment	Date	Solids			DOC Global			DOC (i)		
		UV	PAR	IR	UV	PAR	IR	UV	PAR	IR
Bottom of Surface	9:00	-0.06	-0.02	-0.04	-0.01	-0.02	0.00	0.03	-0.02	0.00
	12:00	-0.03	-0.02	-0.03	0.04	-0.02	0.00	0.04	-0.02	0.00
	15:00	-0.01	-0.02	0.02	0.05	-0.02	0.00	0.02	-0.02	0.00
Top of Subsurface	9:00	0.00	0.00	0.00	0.00	0.00	0.00	0.00	0.00	0.00
	12:00	0.00	0.00	0.00	0.00	0.00	0.00	0.00	0.00	0.00
	15:00	0.00	0.00	0.00	0.00	0.00	0.00	0.00	0.00	0.00
Bottom of Subsurface	9:00	0.02	0.02	-0.30	-0.03	0.03	-0.03	0.00	0.02	-0.03
	12:00	0.03	0.01	0.03	-0.07	0.01	0.00	-0.06	0.01	0.00
	15:00	0.02	0.03	-0.30	-0.03	0.02	-0.03	-0.01	0.02	-0.03

Table 28. Variables Related to Equilibrium Sorption

Variable	Description	Units
$C_{0,i}$	Initial Concentration of Chemical i	mg/L
K_d	Partition Coefficient	L/kg
S_j	Concentration of Solid j	mg/L
C_i^W	Concentration of Dissolved Chemical i	mg/L
C_i^S	Concentration of Sorbed Chemical i	mg/L
V	Volume of Segment	m ³

9.3. Particle Attachment QA/QC

9.3.1. Equilibrium Sorption

Four scenarios tested the equilibrium sorption algorithm in WASP8 and steady state WASP output concentrations were then compared to analytic solutions. Variables used in this section are defined in Table 28. WASP outputs sorbed chemicals in mg of chemical i per kg of total solids, but units have been converted for consistency.

Parameter values as well as output results and percent error for each scenario are shown in Table 29.

9.3.2. Kinetic Sorption

Kinetic sorption algorithms were tested by constructing a WASP model with a single water segment. Sorption process were assumed to occur between chemical and solid in the water segment, with no flow or transport of solids. Two scenarios were tested and the parameters are listed in Table 30.

We tested sorption kinetics in WASP8 with two different scenarios (Table 30). Analytical solutions of these test cases were simulated for comparison and results are presented in Figure 20.

Table 29. Parameter Values and Results for each Scenario

Scenario	Parameter	Variable	Units	Value	WASP output	% Error
1	Initial Concentration of Chemical i	$C_{0,i}$	mg/L	10		
	Partition Coefficient	K_d	L/kg	10		
	Concentration of Solid i	S_j	mg/L	500		
	Concentration of Dissolved Chemical i	C_i^W	mg/L	9.950	9.952	-0.018
	Concentration of Sorbed Chemical i	C_i^S	mg/L	0.050	0.050	-0.020
2	Volume of Segment	V	m ³	100,000		
	Initial Concentration of Chemical i	$C_{0,i}$	mg/L	10		
	Partition Coefficient	K_d	L/kg	10		
	Concentration of Solid i	S_j	mg/L	250		
	Concentration of Dissolved Chemical i	C_i^W	mg/L	9.975	9.976	-0.009
3	Concentration of Sorbed Chemical i	C_i^S	mg/L	0.025	0.025	-0.010
	Volume of Segment	V	m ³	100,000		
	Initial Concentration of Chemical i	$C_{0,i}$	mg/L	10		
	Partition Coefficient	K_d	L/kg	100		
	Concentration of Solid i	S_j	mg/L	250		
4	Concentration of Dissolved Chemical i	C_i^W	mg/L	9.756	9.757	-0.009
	Concentration of Sorbed Chemical i	C_i^S	mg/L	0.244	0.244	-0.010
	Volume of Segment	V	m ³	100,000		

Table 30. Sorption Kinetic Constants and Analytical Errors of Two Scenarios

Scenario	Parameter	Variable	Units	Value	% Error
1	Initial chemical concentration	C_0^W	mg/L	5	0
	Suspended solid concentration	C^S	mg/L	5	
	Sorption rate constant	k_{for}	L/mg-d	0.05	
	Desorption rate constant	k_{rev}	d-1	0.005	
2	Initial chemical concentration	C_0^W	mg/L	15	0

Table 30. Sorption Kinetic Constants and Analytical Errors of Two Scenarios (continued)

Scenario	Parameter	Variable	Units	Value	% Error
	Suspended solid concentration	C^S	mg/L	5	
	Sorption rate constant	k_{for}	L/mg-d	0.01	
	Desorption rate constant	k_{rev}	d-1	0.005	

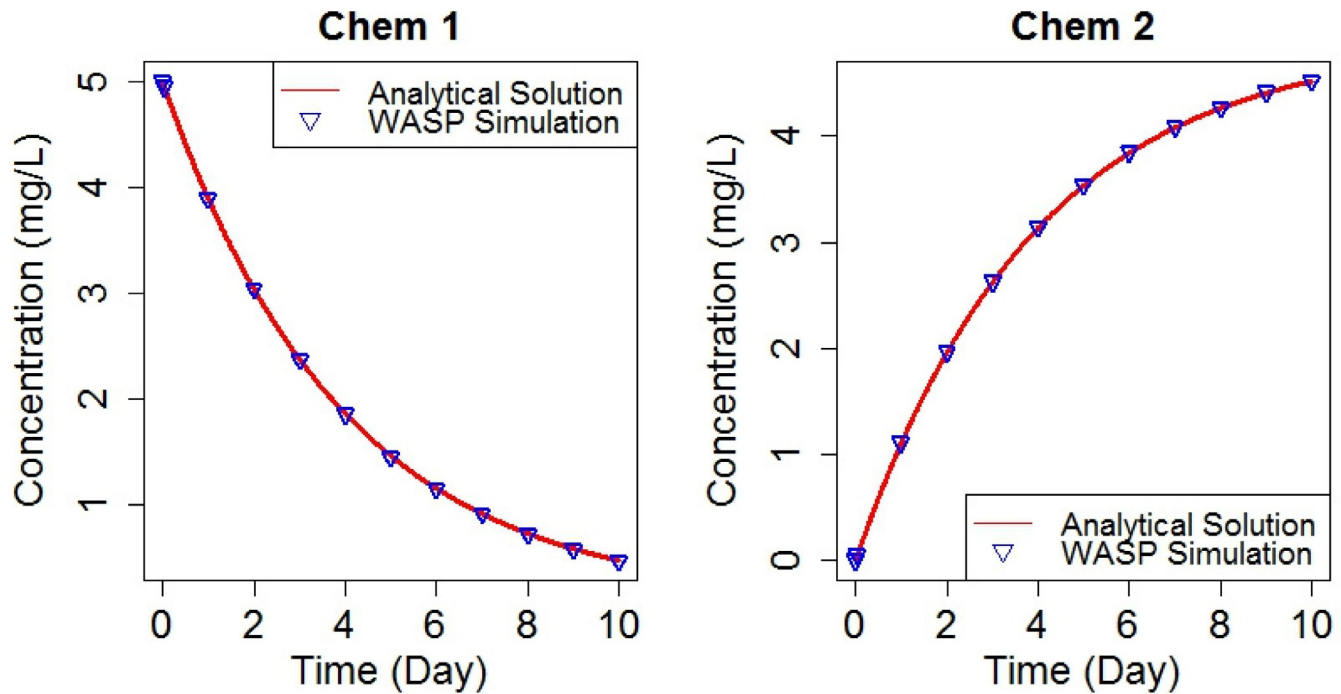


Figure 20. Comparison of Analytical Solution and WASP Simulation for Sorption Kinetics of Scenario 1. Chem 1 represents the freely dissolved chemical concentration, and Chem 2 represents the chemical concentration sorbed to the suspended solid.

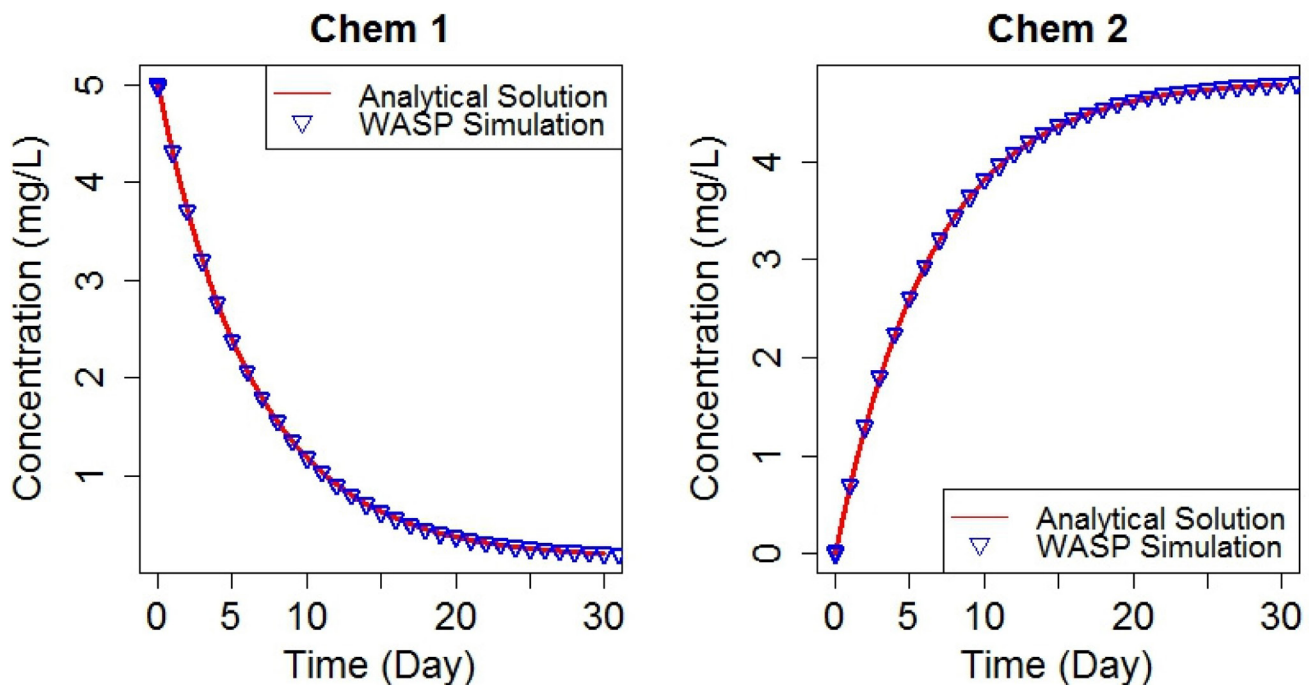


Figure 21. Comparison of Analytical Solution and WASP Simulation for Sorption Kinetics of Scenario 2. Chem 1 represents the freely dissolved chemical concentration, and Chem 2 represents the chemical concentration sorbed on the suspended solid.

Variable	Description	Units	Value
k_b	Boltzmann Constant	$m^2 g s^{-2} K^{-1}$	1.38E-20
T_{water}	Absolute Temperature of Water	K	288.15
G	Shear Rate	s^{-1}	2.00E-05
μ_{water}	Dynamic Viscosity of Water	g/m/s	1.13
g	Gravitational Acceleration on Earth	m/s^2	9.81
S_j^{SPM}	Initial/Boundary Concentration of Solid j	mg/L	100
C_i^{NP}	Initial/Boundary Concentration of Nanoparticle i	mg/L	20
$\rho_{SPM,j}$	Density of Solid j	g/cm^3	2.65
ρ_{water}	Water Density	g/cm^3	1.00
$\rho_{NP,i}$	Density of Nanoparticle i	g/cm^3	1.30
$r_{NP,i}$	Radius of Nanoparticle i	nm	100
$r_{SPM,j}$	Radius of Solid j	mm	8.00E-03
$v_{set,i}^{NP}$	Settling Velocities of Nanoparticle i	m/d	4.99E-04
$v_{set,j}^{SPM}$	Settling Velocities of Solid j	m/d	17.55
Q_{in}	Inflow	m^3/s	Varies
Q_{out}	Outflow	m^3/s	Varies

Table 31. Heteroaggregation Kinetics Parameters

9.3.3. Nanomaterial Heteroaggregation

To test WASP8's heteroaggregation routines, we solved and simulated scenarios for all three components of the ij parameter. Variables used in this section are defined in Table 31.

A WASP model consisting of a single segment simulated the heteroaggregation process between concentrations of nanoparticle i and solid j suspended in the water column.

Table 32. Channel Geometry of WASP Segment

Channel Geometry	
Volume	100,000 m^3
Length	100 m
Depth	10 m
Width	100 m

Table 33 Shows calculated values for $k_{coll,ij}$ and its individual components. For each scenario we varied α as 0.1, 0.01, 0.001, and 1E-6.

Table 33. Calculated Rate of Collision by Mechanism

Component	Calculated Value	Units
Brownian	1.66E-11	m^3/d
Fluid	1.23E-15	m^3/d
Settling	3.62E-9	m^3/d
$k_{coll,ij}$	3.63E-09	m^3/d

We used a concentration of 100 mg/L for S_j^{SPM} and 20 mg/L for C_i^{NP} for all three scenarios. The first used these concentrations as initial conditions; for scenarios two and three, these concentrations are boundary conditions. Scenario 1 used only Brownian motion and was solved dynamically. The second and third scenarios added components of $k_{coll,ij}$ to the first scenario. Scenario 2 incorporates Brownian motion and fluid motion. Scenario 3 incorporates Brownian motion, fluid motion, and differential settling. The second and third scenarios were solved at steady state.

Scenario 1 - Brownian motion only

Scenario 1 looks solely at the effects of the Brownian motion component of $k_{coll,ij}$. It is solved dynamically because the steady state solution would result in zero concentrations.

Initial concentrations of 100 mg/L and 20 mg/L are used for S_j^{SPM} and C_i^{NP} , respectively. The scenario is solved analytically using the mass balance equation:

$$V \frac{\Delta C_i^{NP}}{\Delta t} = Q_{in} C_{in,i}^{NP} - Q_{out} C_i^{NP} - k_{het,ij} C_i^{NP} V \quad \text{Equation 125}$$

We assumed no settling or flows in or out of the system. Therefore, $Q_{in} = 0$ and $Q_{out} = 0$, leaving:

$$\frac{\Delta C_i^{NP}}{\Delta t} = -k_{het,ij} C_i^{NP} \quad \text{Equation 126}$$

From this we can differentiate and solve:

$$C_i^{NP} = C_{0,i}^{NP} e^{-k_{het,ij} t} \quad \text{Equation 127}$$

Table 34 shows calculated $k_{het,ij}$ for different α 's, using an analytic solution. Figure 22 compares the analytic solution and WASP simulation of free nanoparticle and heteroaggregated nanoparticle (Nano-Solid) concentrations, over time when $\alpha = 0.01$.

Table 34. Parameters for Different Cases of α for Brownian Motion Scenario

Parameter	Case 1	Case 2	Case 3	Case 4
$k_{het,ij}$	2.92E-02	2.92E-03	2.92E-04	2.92E-07
α	0.1	0.01	0.001	1.00E-06
N_j^{SPM}	1.76E+10	1.76E+10	1.76E+10	1.76E+10

Scenario 2 - Brownian and fluid motion only

Scenario 2 incorporates Brownian motion and fluid motion; because the two cannot be isolated, we solved them simultaneously. A constant inflow (Q_{in}) and outflow (Q_{out}) of 0.2 m³/s was added to the WASP model. Solid and nanoparticle transport were not included in this scenario. Table 35 shows calculated $k_{het,ij}$ for different alphas using an analytic solution. Solids concentration is set to 100 mg/L.

Table 35. Parameters for Different Cases of α for Brownian Motion and Fluid Motion Scenario

Parameter	Case 1	Case 2	Case 3	Case 4
$k_{het,ij}$	2.92E-02	2.92E-03	2.92E-04	2.92E-07
α	0.1	0.01	0.001	1.00E-06
S_j^{SPM}	100	100	100	100
N_j^{SPM}	1.76E+10	1.76E+10	1.76E+10	1.76E+10

WASP's simulated and analytically solved nanomaterial concentrations for all four alphas are compared in Table 36.

Table 36. Calculated and Simulated Nanoparticle Concentrations Using Different Alphas

Nano Conc [mg/L]	Nano Conc			
	$\alpha = 0.1$	$\alpha = 0.01$	$\alpha = 0.001$	$\alpha = 1E-6$
Analytic Solution	17.11	19.67	19.97	20.00
WASP Simulated	17.11	19.67	19.97	20.00
% Error	0.00	0.00	0.00	0.00

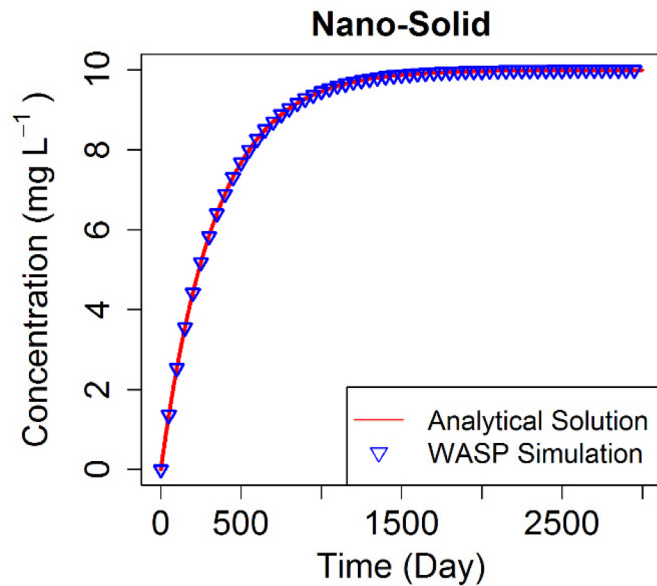
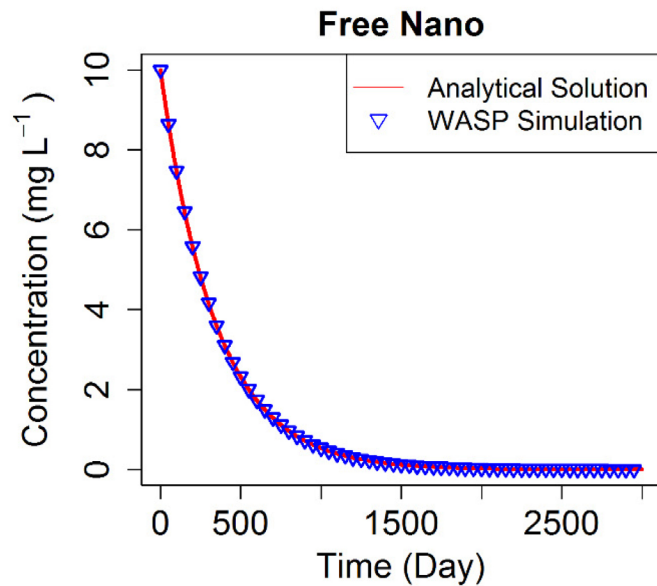


Figure 22. Comparison of Analytical Solution and WASP Simulated Nanoparticle Concentration over Time for Scenario 1

Scenario 3 - Brownian motion, fluid motion, and differential settling.

We add settling into $k_{coll,ij}$. Again, we cannot isolate dynamic settling from other components, so we simulate all three simultaneously. Scenario 3 uses Brownian motion, fluid motion, and differential settling.

Using the steady state equation:

$$V \frac{\Delta S_j^{SPM}}{\Delta t} = Q_{in} S_{in,j}^{SPM} - Q_{out} S_j^{SPM} - v_{set,j}^{SPM} S_j^{SPM} \quad \text{Equation 128}$$

we solve for S_j^{SPM} . By incorporating settling we get a steady state solids concentration of approximately 9 mg/L. Following steps from the previous scenario, we solve for the steady state C_i^{NP} concentration:

$$C_i^{NP} = \frac{Q_{in} C_{in,i}^{NP}}{Q_{out} + k_{het,ij} V} \quad \text{Equation 129}$$

$k_{het,ij}$ constants for different alphas were solved analytically. Parameter values for each case are presented in Table 37.

Table 37. Analytic Solutions for Heteroaggregation Constants Using

Parameter	Case 1	Case 2	Case 3	Case 4
knet,ij	0.573	5.73E-02	5.73E-03	5.73E-06
α	0.1	0.01	0.001	1.00E-06
SjSPM	8.96	8.96	8.96	8.96
NjSPM	1.58E+09	1.58E+09	1.58E+09	1.58E+09

Calculated and simulated free nanoparticle concentrations for all four alphas are shown in Table 38. WASP outputs are within 0.02 percent of the analytic solution.

Table 38. Nanoparticle Concentrations Using Different Alphas

Nano Conc [mg/L]	$\alpha=0.1$	$\alpha=0.01$	$\alpha=0.001$	$\alpha=1E-6$
Analytic Solution	4.63	15.02	19.36	20.00
WASP Simulated	4.63	15.02	19.36	20.00
% Error	-0.02	-0.01	0.00	0.00



Recycled/Recyclable Printed on paper that contains a minimum of 50% post-consumer fiber content processed chlorine free

ISSUE PERMIT NO. G-35



PRESORTED STANDARD
POSTAGE & FEES PAID
EPA
PERMIT NO. G-35

Office of Research and Development (8101R)
Washington, DC 20460

Official Business
Penalty for Private Use
\$300